

The Pennsylvania State University

The Graduate School

College of Engineering

**USING  $\delta^2\text{H}$  AND  $\delta^{18}\text{O}$  TO DETERMINE THE FLOWPATHS AND  
TIMESCALES OF WATER AT THE SUSQUEHANNA SHALE  
HILLS CRITICAL ZONE OBSERVATORY**

A Thesis in

Civil Engineering

by

George H. Holmes III

© 2011 George H. Holmes III

Submitted in Partial Fulfillment

of the Requirements

for the Degree of

Master of Science

August 2011

The thesis of George H. Holmes III was reviewed and approved\* by the following:

Christopher Duffy  
Professor of Civil Engineering  
Thesis Advisor

Elizabeth Boyer  
Associate Professor of Water Resources

Michael N. Gooseff  
Assistant Professor of Civil Engineering

Peggy A. Johnson  
Department Head and Professor of Civil Engineering

\*Signatures are on file in the Graduate School

## ABSTRACT

A stable isotope sampling network was implemented at the Susquehanna Shale Hills Critical Zone Observatory. The objective was to determine the  $\delta^2\text{H}$  and  $\delta^{18}\text{O}$  signature in the catchment pools to determine the flowpaths and timescales of the hydrologic system. The stable isotope network covers all phases of the hydrologic cycle, including precipitation sampled adaptively during precipitation events with an Eigenbrodt NSA-181/S wet-only collector (six-hour samples), soil water sampled weekly along four transects with 80 suction-cup lysimeters, groundwater sampled daily at two wells with ISCO automatic samplers and bi-weekly at 16 wells and stream water sampled daily with an ISCO automatic sampler. The comprehensive sampling of the network was possible because of the DLT-100 liquid water stable isotope analyzer from Los Gatos Research, with a reproducibility of  $\pm 0.2\text{‰}$  for  $\delta^{18}\text{O}$ ,  $\pm 1.0\text{‰}$  for  $\delta\text{D}$  and the capability to run 30 samples per day. The  $\delta^2\text{H}$  and  $\delta^{18}\text{O}$  data showed the dominance of cold season infiltration and recharge, with recharge specifically occurring over the period of late September – May. The  $\delta^2\text{H}$  and  $\delta^{18}\text{O}$  record also showed that groundwater regularly flushed the deep soil water, and that groundwater is the major component of streamflow. Preferential flowpaths in the soil during the cool or non-growing season was identified and is related to stream stormflow. A piecewise constant model for flow, tracer concentration and age was based on the work of Duffy and Cusumano (1998) and Duffy (2010), and was unique in that it solved for transient flow. The finding of the age model was that the mean age of the water in the catchment ranged between 4.5 – 9 months. The oldest ages occurred during the summer drought and the youngest ages occurred during times of maximum recharge over the winter. This research was performed as part of the NSF-funded Critical Zone Observatory and the importance of this effort multi-investigator effort was essential to the success of this research.

## TABLE OF CONTENTS

LIST OF FIGURES.....	v
LIST OF TABLES .....	vi
ACKNOWLEDGEMENTS .....	vii
Chapter 1 Introduction .....	1
Stable Isotope Overview .....	2
$\delta^2\text{H}$ and $\delta^{18}\text{O}$ in Catchment Hydrology .....	4
Age Modeling Theory .....	9
Chapter 2 Site Description and Sampling Methods .....	13
Sampling Methods.....	13
SSHCZO Conceptual Flow Model.....	16
Chapter 3 $\delta^2\text{H}$ and $\delta^{18}\text{O}$ Results .....	19
Meteoric Water Line .....	19
Precipitation .....	22
Soil Water.....	26
Groundwater.....	29
Stream Water.....	32
Chapter 4 $\delta^2\text{H}$ and $\delta^{18}\text{O}$ Discussion .....	35
Chapter 5 Age Model.....	39
Derivation.....	39
Age Model Results and Discussion.....	44
Chapter 6 Conclusion.....	52
References .....	54
Appendix $\delta^2\text{H}$ and $\delta^{18}\text{O}$ Data and Age Model Output .....	59

## LIST OF FIGURES

Figure 2-1: Water sampling locations at the Susquehanna Shale Hills CZO. The contours are 2m apart and the dashed line represents the area constantly saturated by groundwater.....	14
Figure 2-2: Theoretical cross-section of the Shale Hills catchment illustrating the conceptual flowpaths. The cross-section is not drawn to scale.....	18
Figure 3-1: a. Local meteoric water line plot for the Shale Hills $\delta^2\text{H}$ and $\delta^{18}\text{O}$ data. The local (lmwl) and global (gmwl) meteoric water lines are both shown. b. Local meteoric water line plot using the 95% quantile ellipse for each pool. The quantile ellipses were calculated in Mathematica.....	20
Figure 3-2: a. MWL plot showing the precipitation $\delta^2\text{H}$ and $\delta^{18}\text{O}$ grouped by precipitation type. The precipitation type was determined by the lpm. b. Time series of amount weighted event and monthly precipitation $\delta^{18}\text{O}$ and the precipitation amount (mm).....	24
Figure 3-3: a. MWL plot of the soil water $\delta^2\text{H}$ and $\delta^{18}\text{O}$ grouped by depth region. b.. Average $\delta^{18}\text{O}$ plotted by depth. The red lines are confidence intervals equal to $\pm$ one standard deviation. The location of the groundwater and precipitation $\delta^{18}\text{O}$ is shown for comparison.....	27
Figure 3-4: a. Local meteoric water line plot of the groundwater $\delta^2\text{H}$ and $\delta^{18}\text{O}$ data. b. Time series plot of the groundwater $\delta^{18}\text{O}$ record and groundwater depth below the surface (m).....	30
Figure 3-5: a. Local meteoric water line plot of the stream water $\delta^2\text{H}$ and $\delta^{18}\text{O}$ data. b. Time series plot of the stream water $\delta^{18}\text{O}$ and the discharge ( $\text{m}^3/\text{s}$ ).....	33
Figure 4-1: Picture of a preferential flowpath emptying directly into the stream from the North bank at the SSHCZO.....	38
Figure 5-1: a. The solution to the piecewise constant inputs age model, for the case of a constant input. b. The solution to the piecewise constant inputs age model for the case of a pulse input. c. The solution to the piecewise constant inputs age model for the case of an oscillating input. ....	41
Figure 5-2: The discharge-volume relationship for the Shale Hills data. The discharge and volume data come from the PIHM model (Qu and Duffy, 2007), which was run using 32 years of forcing data. The data plotted are monthly means from 2009 and 2010.....	45

Figure 5-3: a. The solution to the piecewise constant inputs age model using the Shale Hills data. a. The modeled flow plotted with the measured flow. b. The modeled  $\delta^2\text{H}$  and  $\delta^{18}\text{O}$  concentrations plotted with the measured  $\delta^2\text{H}$  and  $\delta^{18}\text{O}$  concentrations. c. The mean age of the water stores in the system determined from the  $\delta^2\text{H}$  and  $\delta^{18}\text{O}$ .....49

## LIST OF TABLES

Table <b>3-1</b> : $\delta^2\text{H}$ and $\delta^{18}\text{O}$ averages and other statistical parameters for the Shale Hills data. The precipitation average is weighted by the amount of precipitation..	22
Table <b>5-1</b> : The monthly mean data used for the piecewise constant inputs age model for the SSHCZO.	46

## ACKNOWLEDGEMENTS

First and foremost I would like to acknowledge my wife Stephanie. Without her support I would have never made it to this point. She put up with more than her fair share and I love her more than anything for it. I would also like to thank my parents for their guidance. They were always there to listen and help point me in the right direction.

I would like to thank Dr. Christopher Duffy for giving me this wonderful opportunity. I enjoyed all of the time I spent working with him, and I am astonished at what we were able to accomplish. Finally I would like to thank all of the friends I made working at Shale Hills and also in the office. I thought being a graduate student would be all work and no play, but instead we were able to have many great times together.

## Chapter 1

### Introduction

The Susquehanna Shale Hills Critical Zone Observatory (SSHCZO) was designed for the ultimate goal of determining the formation, evolution and function of regolith. The functioning of regolith affects the hydrologic flowpaths and timescales of the water in a catchment (Anderson et al., 2008; Brantley et al., 2007). Hydrologic studies have occurred at Shale Hills since the 1970s focusing on streamflow generation (Lynch, 1976; Duffy, 1996) soil moisture and preferential flow (Lin, 2006; Lin et al., 2006; Lin and Zhou, 2008; Graham and Lin, 2011) and solute transport (Jin et al., 2010; Jin et al., 2011; Kuntz, 2010). These studies have found that the streamflow largely depends on the antecedent soil moisture and groundwater, which is why the stream does not flow over the summer growing season due to low soil moisture and a low water table (Lynch, 1976). Once the soil moisture deficit is satisfied than groundwater recharge can occur over the cold season or non-growing season (Deines et al., 1990; O'Driscoll et al., 2005). Subsurface water is transported through several preferential flowpaths at Shale Hills (Lin, 2006; Lin et al., 2006; Lin and Zhou, 2008), and the groundwater regularly flushes the deep soil water (Lynch and Corbett, 1989; Duffy, 1996). A conceptual hydrologic model can be pieced together from these studies but no study has looked at the hydrology as a whole. The goal of this research is to identify the composition of the hydrologic pools and the flowpaths and timescales through the catchment and to evaluate how these pools interact and mix to form runoff within the watershed. To accomplish this an isotopic sampling network was developed for the collection of  $\delta^2\text{H}$  and  $\delta^{18}\text{O}$  samples.  $\delta^2\text{H}$  and  $\delta^{18}\text{O}$  were chosen because they are conservative tracers at low temperatures (Hoefs, 2009) and they compose the water molecule. The age of the hydrologic system was determined by modeling the flow and isotopic concentration of the stream. The

model used was created by Duffy (2010), and was chosen because it is the first of this type of model to solve for transient flow.

### Stable Isotope Overview

Isotopes are measured as a ratio of the heavy (rare) to light (common) isotope, e.g.  $R = {}^2\text{H}/{}^1\text{H}$  or  ${}^{18}\text{O}/{}^{16}\text{O}$ . Measuring the exact ratio of a sample is inaccurate because the heavy isotopes are not abundant, instead it is orders of magnitude more accurate to relate the ratio of a sample to a known ratio of standard. The standard used for water is Vienna Standard Mean Ocean Water (VSMOW), and the absolute abundance of deuterium ( ${}^2\text{H}$  or D) in VSMOW is  ${}^2\text{H}/{}^1\text{H} = 155.95 \times 10^{-6}$  (Dewit et al., 1980), and  ${}^{18}\text{O}$  is  ${}^{18}\text{O}/{}^{16}\text{O} = (2005.2 \pm 0.45) \times 10^{-6}$  (Baertschi, 1976). Isotope values are reported in delta ( $\delta$ ) notation

$$\delta_{\text{sample}} = \left[ \frac{R_{\text{sample}} - R_{\text{standard}}}{R_{\text{standard}}} \right] \times 1000$$

and the values are on a permil (‰) scale. A positive  $\delta$  is enriched in the heavy isotope compared to the standard and a negative  $\delta$  is depleted in the heavy isotope compared to the standard.

The abundance of stable isotopes varies in nature due to fractionation. Fractionation occurs because of differences in mass between isotopes, which causes the isotopes to have different physiochemical properties. The physical properties of an isotope affect its vibrational motions only, therefore causing differences in zero-point energies of isotopes (Hoefs, 2009). Therefore it is harder to break a bond between two  ${}^2\text{H}$  isotopes than it is between two  ${}^1\text{H}$  isotopes, because the bond of the light isotope is weaker. Fractionation is significant at low temperatures and disappears at higher temperatures because of the amount of energy available. Fractionation is measured using the fractionation factor,  $\alpha$ , or epsilon,  $\epsilon$ .

$$\alpha_{A-B} = \frac{R_A}{R_B} \approx \frac{1000 + \delta_A}{1000 + \delta_B}$$

$$\varepsilon_{A-B} = (\alpha_{A-B} - 1) \times 1000$$

Fractionation is important for light isotopes because of larger mass differences. For example, using the atomic weights of Sharp (2007),  $^2\text{H}$  is 99.8% heavier than  $^1\text{H}$ ,  $^{18}\text{O}$  is 12.5% heavier than  $^{16}\text{O}$ , but a heavier isotope like  $^{238}\text{U}$  is only 1.27% heavier than  $^{235}\text{U}$ .

Fractionation occurs as either an equilibrium or kinetic reaction (Hoefs, 2009).

Equilibrium fractionation occurs when the compound is in a closed environment and the products and reactant are able to reach isotopic equilibrium. The backwards and forwards reaction rates are equal, and the  $\delta$  value in each compound reaches a constant value. In equilibrium fractionation it is generally understood that the heavy isotopes will preferentially accumulate in the denser state (eg. solid>liquid>vapor).

Kinetic fractionation is an irreversible process, meaning that the backwards and forwards reaction rates are not equal. This can be due to the products being isolated from the reactants or the products being carried away from the reactants, like in the case of evaporation. The amount of fractionation depends on the ratio of masses of the isotopes in the products and reactants and their bond strengths. It is generally understood that during kinetic fractionation the light isotopes accumulate in the products because it takes less energy to break their bonds.

The most important fractionations with respect to water are related to phase changes, due to differences in vapor pressure and freezing point (Friedman et al., 1964). Water molecules containing  $^{18}\text{O}$  and  $^2\text{H}$  cause the water to have a lower vapor pressure and freezing point, therefore preferentially accumulating in the more dense phases.

When studying the stable isotopes of water it is only necessary to consider water molecules of the form  $^1\text{H}_2^{16}\text{O}$ ,  $^1\text{H}^2\text{H}^{16}\text{O}$ , and  $^1\text{H}_2^{18}\text{O}$ . This is because these forms occur in

concentrations that are orders of magnitude larger than the concentrations of the other six forms of the water molecule (Friedman et al., 1964).

### **$\delta^2\text{H}$ and $\delta^{18}\text{O}$ in Catchment Hydrology**

$\delta^2\text{H}$  and  $\delta^{18}\text{O}$  isotopes are ideal in catchment studies because the isotopes fractionate and mix as they move between the different pools in the catchment. This has led to  $\delta^2\text{H}$  and  $\delta^{18}\text{O}$  being used for hydrograph separations (Skalsh et al., 1976; Sklash and Farvolden, 1979; Rice and Hornberger, 1998), estimation of soil water movement and evaporation (Allison and Barnes, 1983; Barnes and Allison, 1988; Gazis and Feng, 2004), estimation of groundwater composition and recharge (Gat 1971; Davisson and Criss, 1993; Criss and Davisson, 1996; Darling and Bath, 1988; Winograd et al., 1998) and the determination of preferential flowpaths and the old water paradox (McDonnell, 1990; Leaney et al., 1993; Kirchner, 2003; Vogel et al., 2010). It is necessary to understand how  $\delta^2\text{H}$  and  $\delta^{18}\text{O}$  function in catchments so that these isotopes can be used for these purposes.

Precipitation is the only input to the SSHCZO, so the  $\delta^2\text{H}$  and  $\delta^{18}\text{O}$  signature of precipitation serves as the starting point for the  $\delta^2\text{H}$  and  $\delta^{18}\text{O}$  signature that will be acquired by the soil water, groundwater and stream water. The main factors controlling the  $\delta^2\text{H}$  and  $\delta^{18}\text{O}$  of a precipitation event is the source of water, temperature during condensation, fraction of original water remaining, amount of recycled (evapotranspired) water, pathway of the event and isotopic exchange of water droplets and water vapor.

The source water region is important because of the temperature and relative humidity at the time of evaporation. A higher temperature will decrease the fractionation factor while the relative humidity determines the amount of evaporation and exchange between the water vapor and liquid water (Merlivat and Jouzel, 1979). Evaporation is a kinetic fractionation process, and

the water vapor is always depleted in  $\delta^2\text{H}$  and  $\delta^{18}\text{O}$  relative to the liquid water (Dansgaard, 1964). The water vapor receives more  $\delta^2\text{H}$  than  $\delta^{18}\text{O}$  though because it weighs less and therefore takes slightly less energy to break the bond.

Condensation is an equilibrium fractionation process where the amount of fractionation is controlled by the air temperature (Dansgaard, 1964). Because of this the  $\delta^2\text{H}$  and  $\delta^{18}\text{O}$  of precipitation correlates with temperature on a global scale (Dansgaard, 1964; Siegenthaler and Oeschger, 1980; Lawrence, 1980; Rozanski et al., 1992). Since condensation is an equilibrium process, theoretically the initial condensate will have the same composition as the source water, but this is not the case due to kinetic evaporation (Dansgaard, 1964).

As condensation continues on a finite volume of water vapor, the heavy isotopes become depleted in the water vapor because they are more stable in the liquid water. This leads to four 'effects', which were discovered by Dansgaard (1964) and Friedman et al. (1964). They are the amount effect, continental effect, latitude effect and altitude effect. The premise behind all of the effects is that lower temperatures and a finite volume of water vapor lead to increased fractionation, which occurs as a spatial or temporal gradient as rainout occurs, or an air mass moves over the continent, etc.

Precipitation isotopic values are also influenced by the amount of water evapotranspired back to the air mass. Concentration gradients calculated for the Amazon basin show a reduced 'continental effect' when compared to other regions (Araguas-Araguas et al., 2000). Unlike evaporation transpiration does not fractionate water so the water vapor returning to the air mass is comparatively enriched.

During decent liquid precipitation is subject to isotopic alteration by evaporation and isotopic exchange with atmospheric moisture. Evaporation occurs at the beginning of a precipitation event, because the atmosphere underneath the air mass is normally not saturated with water, and after saturation of the underlying air isotopic exchange occurs. The amount of

time or distance it takes for a water drop to isotopically equilibrate with the atmosphere is positively related to the drop radius and the atmospheric temperature (Friedman et al., 1962). It should be noted that during heavy rain, it is the liquid component that dominates the exchange process causing the atmospheric water vapor to have the same  $\delta^2\text{H}$  and  $\delta^{18}\text{O}$  as the liquid (Dansgaard, 1964). Isotopic exchange also affects other open water bodies. The rate of exchange is controlled by the volume and surface area of the water bodies (Ingraham and Criss, 1993). In a study using beakers of different volume and surface area Ingraham and Criss found differences of up to 9% of the original isotopic composition after five days.

The pathway of a precipitation event determines the conditions under which condensation will occur. In a study of precipitation  $\delta^2\text{H}$  and  $\delta^{18}\text{O}$  and the pathway of the events at Mohonk, NY, Lawrence et. al (1982) found a distinct difference among the isotopic signatures and the corresponding path of the precipitation event. Their finding was that as the center of the storm is displaced seaward the  $\delta^2\text{H}$  of the precipitation decreases. The reason for the decrease is because the frontal surface creating these events is at a higher altitude when the storms are seaward.

Isotopic values of precipitation also vary during a storm. Pionke and DeWalle (1992) collected precipitation samples over 21 minute intervals for 33 storms in central Pennsylvania and found that short storms showed little change in the  $\delta^2\text{H}$  and  $\delta^{18}\text{O}$ , but long storms showed great variability that seemed to be related to precipitation intensity. Differences in  $\delta^{18}\text{O}$  of 15‰ were found for an 11-hour storm that dropped 31 mm of precipitation. This intra-storm variability is important because a specific part of the storm may dominate the hydrologic response of the catchment.

Precipitation  $\delta^2\text{H}$  and  $\delta^{18}\text{O}$  is variable because it is a global scale process, but this variation is attenuated in the other hydrologic pools. Generally the soil water, groundwater and stream water pools are isotopically affected by fractionation from evaporation and freeze/thaw and mixing with water bodies that have a different  $\delta^2\text{H}$  and  $\delta^{18}\text{O}$  signature. Evaporation enriches

the  $\delta^2\text{H}$  and  $\delta^{18}\text{O}$  signature of water, freezing depletes the  $\delta^2\text{H}$  and  $\delta^{18}\text{O}$  signature in liquid water and melt water gradually enriches the  $\delta^2\text{H}$  and  $\delta^{18}\text{O}$  signature. Freezing and melting are both kinetic fractionation processes but they leave no permanent change on the  $\delta^2\text{H}$  and  $\delta^{18}\text{O}$  composition as long as all of the water is frozen or melted.

There are many ways that  $\delta^2\text{H}$  and  $\delta^{18}\text{O}$  signatures can be used to understand the hydrologic functioning of a catchment. Hydrograph separations are possible because of the difference between precipitation  $\delta^2\text{H}$  and  $\delta^{18}\text{O}$  and that of the soil water, groundwater and stream water. Sklash et al. (1976) and Sklash and Farvolden (1979) used a simple linear two-component mixing model to determine the relative contributions to streamflow from event and pre-event water. Pre-event water was any water found in the catchment before the precipitation event while the event water was the precipitation. These studies were the first to show that pre-event water, the groundwater and soil water, made up the bulk of the streamflow during a precipitation event. More recent studies have used three-component and even five-component models, by using additional tracers, to determine the relative contributions of soil water, groundwater and precipitation (Rice and Hornberger, 1998; Brown et al., 1999; Uhlenbrook and Hoeg, 2003; Sayama and McDonnell 2009).

The finding that pre-event water contributes the majority of water to the stream during a storm has led to the old water paradox (Kirchner, 2003). The paradox is that during a precipitation event “old” subsurface water is quickly mobilized and forms the bulk of the streamflow, rather than the precipitation falling on the catchment. So far scientists have tried to explain why this water is mobilized and not the event water, and McDonnell (1990) even used  $\delta^2\text{H}$  for his study. McDonnell’s hypothesis was that the old water was quickly transported to the stream through macropores. The reason that the bulk of the water was old water was because the soil was almost completely saturated. Therefore he argued that it only took a small amount of

event water to saturate the soil and initiate macropore flow. The old water paradox still puzzles scientists, despite many attempts to explain it.

$\delta^2\text{H}$  and  $\delta^{18}\text{O}$  have proven useful in estimating subsurface evaporation and flowpaths. Allison and Barnes (1983) modeled soil water evaporation using the enrichment of  $\delta^2\text{H}$  and showed that evaporation typically occurs in the top one meter of soils. It is possible to trace the movement of soil water due to isotopically distinct precipitation events. The infiltrated precipitation serves as an isotopic tag that can be followed and used to determine infiltration and recharge rates and soil water flowpaths (Barnes and Allison, 1988; Bengtsson et al., 1987; Darling and Bath, 1988; Gazis and Feng, 2004).  $\delta^2\text{H}$  and  $\delta^{18}\text{O}$  have also been used to understand the functioning of preferential flowpaths and mobile and immobile water (McDonnell, 1991; Leaney et al. 1993; Vogel et al., 2010; Brooks et al., 2010). In particular, Leaney et al. (1993) found that water travelling through preferential flowpaths was bypassing parts of the soil column and contributing a large portion of water to streamflow. Brooks et al. (2010) have also found that mobile and immobile water have different  $\delta^2\text{H}$  and  $\delta^{18}\text{O}$  signatures, which could change the way the unsaturated zone is conceptualized.

$\delta^2\text{H}$  and  $\delta^{18}\text{O}$  have also been used to investigate groundwater flowpaths and the timing and constituents of recharge water (Gat, 1971). Davisson and Criss (1993) were able to show that the composition of recharge changed over the course of the year depending on the relative height of the groundwater. Winograd et al. (1998) were also able to determine the make up of groundwater recharge by determining the precipitation  $\delta^2\text{H}$  and  $\delta^{18}\text{O}$  seasonal signatures.

$\delta^2\text{H}$  and  $\delta^{18}\text{O}$  in hydrologic studies are normally plotted on a meteoric water line plot (mwl). Craig (1961) was the first to plot  $\delta^2\text{H}$  vs  $\delta^{18}\text{O}$  for water samples collected around the world and find that  $\delta^2\text{H}$  and  $\delta^{18}\text{O}$  are linearly related. The linear relationship formed by global precipitation samples is called the global meteoric water line and has the relationship

$$\delta^2\text{H} = 8\delta^{18}\text{O} + 10.$$

Local precipitation samples will have a slightly different linear relationship, and they are called local meteoric water lines. The significance of the lmwl is that fractionated water samples do not plot along the lmwl. Evaporated samples plot below the lmwl because slightly more  $\delta^2\text{H}$  is evaporated relative to  $\delta^{18}\text{O}$  (Hoefs, 2009). Snowmelt plots above the lmwl because slightly more  $\delta^2\text{H}$  is melted relative to  $\delta^{18}\text{O}$  (Clark and Fritz, 1997). Therefore the mwl plot is essential to the interpretation of  $\delta^2\text{H}$  and  $\delta^{18}\text{O}$  data from catchment waters.

### **Age Modeling Theory**

The theory of age and residence time modeling for watersheds was developed through the early work of chemical engineers modeling tank reactors (Danckwerts, 1953; Nauman, 1969, 1973). Eriksson (1971) and Bolin and Rodhe (1973) gave concise summaries of the reservoir theory, which brought the theory of age modeling clearly into the field of hydrology. The premise behind the reservoir theory is that an element entering a well-mixed reservoir is characterized by  $\tau$ , the time that has elapsed since it entered the reservoir. The elements are then arranged in a cumulative function  $M(\tau)$ , or  $F(\tau)$  for the flux leaving the reservoir, which is the total mass of elements in the reservoir that has spent a time equal to or less than  $\tau$  in the reservoir.  $M(\tau)$  or  $F(\tau)$  can be thought of as the residence time distribution (rtd), which gives the distribution of residence times for all of the elements in the reservoir. Then the steady-state mean residence time or turnover time is defined as  $\tau_0 = M_0/F_0$ , the total mass divided by the total flux. The average age of elements in the reservoir is defined as

$$\tau_a = \frac{1}{M_0} \int_0^{\infty} \tau dM(\tau).$$

The rtd of a reservoir is important because a mean residence time can be achieved many ways, so the rtd shows how the reservoir is unique. The reservoir theory only applies to the steady state flow case, as do most age models.

Maloszewskie and Zuber (1982) introduced several lumped parameter models for the determination of the residence time from isotope data. The convolution integral was used along with a weighting function that specified how the isotope moved through the system:

$$C_{out}(t) = \int_{-\infty}^t C_{in}(\tau) \exp[-\lambda(t - \tau)] g(t - \tau) d\tau$$

where  $C_{out}$  and  $C_{in}$  are the output and input concentrations,  $\tau$  is the transit time of the isotope,  $\lambda$  is the half-life for a radioactive isotope, and  $g$  is the weighting function. There are several weighting functions that can be used including piston flow, exponential flow, combined exponential and piston flow, and dispersive flow. The correct weighting function is chosen by matching the modeled output concentration to the measured output concentration. The transit time or age of the tracer for this model was defined as

$$\tau = \frac{\int_0^{\infty} tC(t) dt}{\int_0^{\infty} C(t) dt}$$

The convolution integral has been widely used even though there are several drawbacks. First is that it is difficult to accurately define the input concentration, and the input is supposed to be instantaneous. Bergmann et al. (1986) developed an equation for the input function that uses  $\alpha$ , an infiltration coefficient, to better define the input concentration. A second problem is that this model assumes steady state flow, which is not found in nature. Werner and Kadlec (1996) show that the output concentration from a system depends on when the tracer entered the system relative to the flow through the system. To get around this problem they use a flow-weighted time, which weights the instantaneous volume by the total volume that leaves the system during the period of interest. Zuber (1986) also got around the steady state assumption by rewriting the lumped parameter model equations using the tracer mass flux. He notes though that this can only work for catchments with short residence times because a longer input and output concentration

time series is required. The general lumped parameter model can also not deal with mobile and immobile flow and preferential flow. The advantage of the lumped parameter model of Maloszewski and Zuber (1982) is that it gives the rtd of the water rather than just a mean residence time.

Goode (1996) was able to directly simulate the age of groundwater by developing an advective – dispersive equation that conserves the conceptual “age mass”. Age mass is defined as the mean age of a parcel of water multiplied by the mass of the water parcel. Therefore when two water bodies mix the age is a mass-weighted average of the two water bodies. More recently Delhez et al. (1999) and Gourgue et al. (2006) have shown that by using age mass it is possible to analyze the moments of the concentration equation without actually needing to define the exact form of the equation. This allowed Duffy (2010) to develop a coupled dynamical system of differential equations that include transient flow and a theoretical approach to tracer age that does not require the residence time functional form, only the first 2 moments. The system of equations was formed from general equations of flow and concentration for a volume averaged system. The total fluid volume of the system satisfied a balance equation:

$$\frac{dV}{dt} = Q_{in} - Q_{out}$$

and a tracer mass balance equation:

$$\frac{dVC}{dt} = Q_{in} C_{in} - Q_{out} C_{out} + V\Gamma_c$$

where  $\Gamma_c$  represents the internal sources and sinks for the tracer. The final dynamical set of equations that came from the balance equations are:

$$\frac{dV}{dt} = Q_{in} - Q_{out}$$

$$\frac{dC}{dt} = \frac{Q_{in}}{V} (C_{in} - C_{out}) + \Gamma_c$$

$$\frac{d\alpha}{dt} = C_{out} - \frac{Q_{in}}{V}\alpha + \Gamma_{\alpha}$$

where  $\alpha$  is the age concentration. The tracer mean age is defined as

$$A(t) = \frac{\alpha(t)}{C(t)}.$$

Duffy (2010) extended the dynamical system to include mobile and immobile flow, which have been shown to be isotopically distinct (Brooks et al., 2010).

## Chapter 2

### Site Description and Sampling Methods

The SSHCZO is a forested, 19.8-acre catchment located in Central Pennsylvania approximately 12 miles southwest of State College (Figure 2-1). The catchment is v-shaped with an average slope of 18 and 16 degrees for the north and south ridges respectively (Lynch, 1976). The slopes are populated with deciduous trees (maple, oak, beech) and the valley is populated with coniferous trees (hemlock, pine) (Lin et al., 2006). The entire catchment is underlain by Rose Hill Formation (Clinton Group) shale with interbedded limestone (Lynch, 1976). The strike and dip of the bedrock is approximately Northeast-Southwest and 75 degrees to the Northwest. Average soil thickness is 1.4m with larger thicknesses in the valleys and swales and smaller thicknesses on the slopes and ridge-top (Lin et al., 2006). There are five main soil series in the catchment, Weikert, Berks, Rushtown, Blairton and Ernest (Lin et al., 2006). The catchment contains a first order stream that typically does not flow from mid-June to mid-September. The catchment receives approximately 995 mm of precipitation annually, with winter precipitation in the form of snow.

### Sampling Methods

Precipitation is measured at a weather station using an Ott-Pluvio weighing type rain gauge and a Thies Clima Laser Precipitation Monitor (LPM) (Figure 2-1). The LPM differentiates types of precipitation (eg. light/moderate/heavy rain, snow, hail) by the diameter of the drops, air temperature and the precipitation intensity. The weather station also has instruments recording temperature, relative humidity, wind direction and speed, net radiation and

snow depth. Soil moisture is measured manually by depth at approximately 80 locations using a time-domain reflectometer probe (Lin et al., 2006). Groundwater height is measured every ten minutes at three wells (RTH1-RTH3), and manually every two weeks (Well2-Well18).

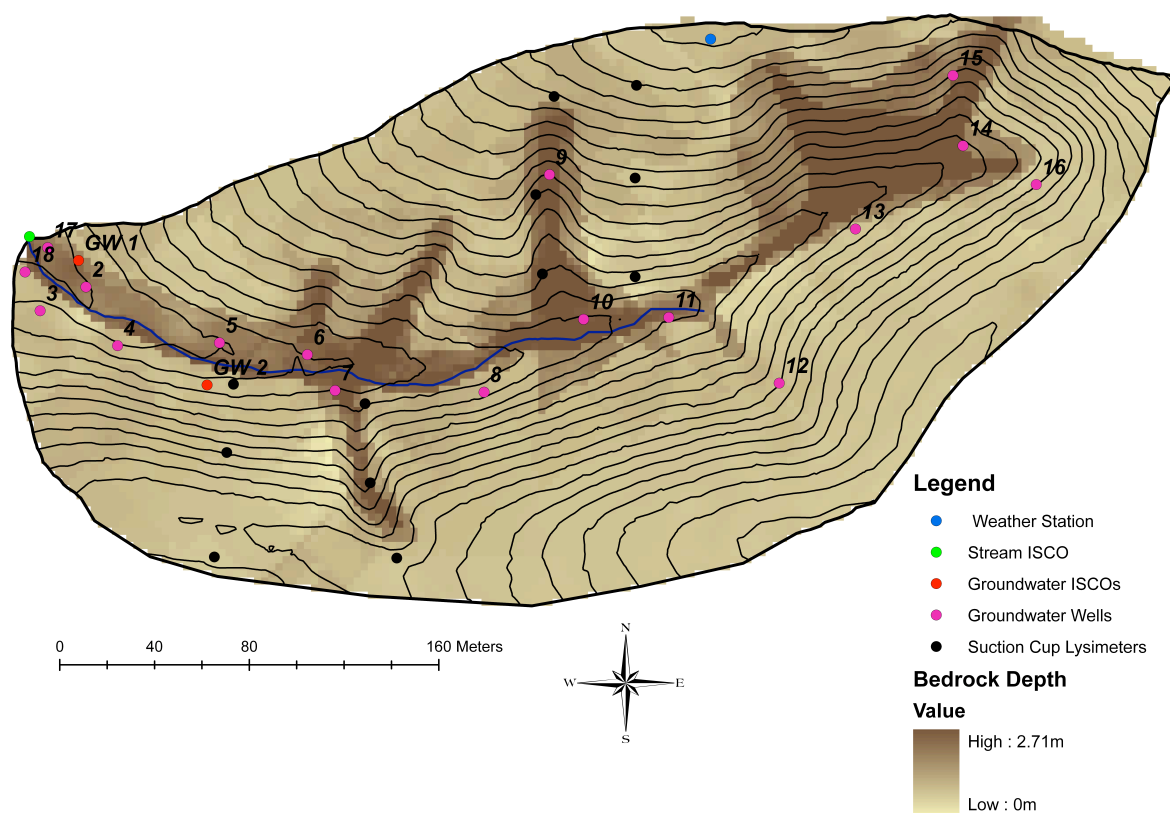


Figure 2-1: Water sampling locations at the Susquehanna Shale Hills CZO. The contours are 2m apart and the dashed line represents the area constantly saturated by groundwater.

Water samples for  $\delta^2\text{H}$  and  $\delta^{18}\text{O}$  were collected in 30mL amber glass vials with polyseal cone-lined phenolic caps to prevent evaporation. Precipitation samples were collected from an Eigenbrodt wet only precipitation collector (model NSA 181/S), located at the weather station. The NSA 181/S has a gold plated sensor that opens the instrument only when there is precipitation. The NSA 181/S contains eight 1L bottles that are separated into two groups of

four. Each group of bottles collects precipitation for user specified duration of time. For the present research the first bottle collected for 30 minutes and the following three bottles collected for six hours each. Soil water samples were collected every two weeks from suction cup lysimeters (Soilmoisture 1900 series). The lysimeters were grouped into four transects, two each on the north and south slopes, and each slope had one transect in a swale and one transect on the planar hill slope. The lysimeters in each transect were grouped into three clusters, one at the ridge-top, mid-slope and valley floor. In each cluster lysimeters were positioned from the soil surface to the bedrock with spacing's of 10 - 20cm. Groundwater samples were collected daily using an ISCO automatic sampler at two locations (GW1 and GW2). The wells that these samples were collected from are approximately nine feet deep and are not screened. Additional groundwater samples were collected every two weeks from 17 wells (Well 2-Well18). These wells vary in depth from 10ft to 17ft, and have a four-foot screen at the base of each well. Stream water was collected daily at the outlet using an ISCO automatic sampler.

The analysis for  $\delta^2\text{H}$  and  $\delta^{18}\text{O}$  was performed on a DLT-100 liquid-water stable isotope analyzer from Los Gatos Research. The instrument uses a unique kind of laser absorption spectrometry termed Off-Axis Integrated Cavity Output Spectrometry (off-axis ICOS). The DLT-100 is able to analyze 30 unknown samples every 24 hours, with a precision of  $\pm 0.6\%$   $\delta^2\text{H}$  and  $\pm 0.2\%$   $\delta^{18}\text{O}$  (Lis et al., 2008). The standards used during analysis were calibrated on the VSMOW-2/GISP-2 scale. To account for instrumental drift the unknown samples were positioned between groups of known standards. The standards on either side of the unknowns were used to calculate the  $\delta$  of the unknowns. To account for memory effects, since the same apparatus is always used, every sample was analyzed six times and the last four measurements were averaged together and used as the reported  $\delta$ .

## SSHCZO Conceptual Flow Model

Hydrologic studies have taken place at Shale Hills since the 1970's when Lynch (1976) performed an artificial irrigation experiment to determine the affect of antecedent soil moisture on stream flow generation. Since then several other experiments have been performed in the catchment that have advanced the understanding of the hydrology, and will serve as the basis for the SSHCZO conceptual flow model (Figure 2-2).

Shale Hills contains a first-order stream that generally flows from October to June except for extremely cold periods with deep frost. From late June to mid-September transpiration utilizes a large portion of the soil water and shallow groundwater. This four-month span accounts for 30% of the annual precipitation of which almost none produces significant recharge. Other studies in Central Pennsylvania have reached the same conclusion, using  $\delta^2\text{H}$  and  $\delta^{18}\text{O}$  to show that recharge rarely occurred over the summer growing season (O'Driscoll et al., 2005; Deines et al., 1990). In late September and October decreasing evapotranspiration and heavy rains saturate the soil water and increase recharge to the groundwater. Low temperatures during the winter freeze the ground, reducing infiltration and lowering the water table below the channel in some years. Recharge is reinitiated only when temperatures are above freezing for a period of time sufficient to thaw the ground and melt snow. In the spring recharge will continue until evapotranspiration prevents vertical soil water flow.

Preferential flow paths in soils are known to exist at Shale Hills (Lin et al., 2006, Lin, 2006; Lin and Zhou, 2008; Graham and Lin, 2011), and salt tracer experiments have shown that 30 – 50% of the pore space is composed of mobile pores (Kuntz, 2010). Lateral flow along the A/B soil interface and the soil/bedrock interface occurs due to a decrease in the vertical hydraulic

conductivity. Macropore's, likely from animal burrows and tree roots, transport water in the soil column vertically, and return flow occurs in the valley due to the soil in this region becoming fully saturated during large precipitation events.

It has been observed at Leading Ridge, an experimental watershed across the valley from Shale Hills, and hypothesized at Shale Hills, that groundwater periodically rises and flushes the soil water (Lynch and Corbett, 1989; Duffy, 1996). Lynch and Corbett (1989) showed that groundwater flushing was responsible for an odd pattern of streamflow sulfate concentrations. They found that sulfate was stored in the soil water during periods of low soil moisture. In the spring the groundwater was recharged and flushed the sulfate that was stored in the soil. Duffy (1996), modeling groundwater flow at Shale Hills, showed that shallow groundwater lenses develop on the hill slopes after large precipitation events. These lenses move laterally down slope removing the soil water that previously occupied the same space.

There is minimal overland flow at Shale Hills, so stream water flow and chemistry is dominated by soil- and groundwater. This research will use the  $\delta^2\text{H}$  and  $\delta^{18}\text{O}$  record to estimate the relative contributions, pathways and timing of runoff at the Shlae Hills site.

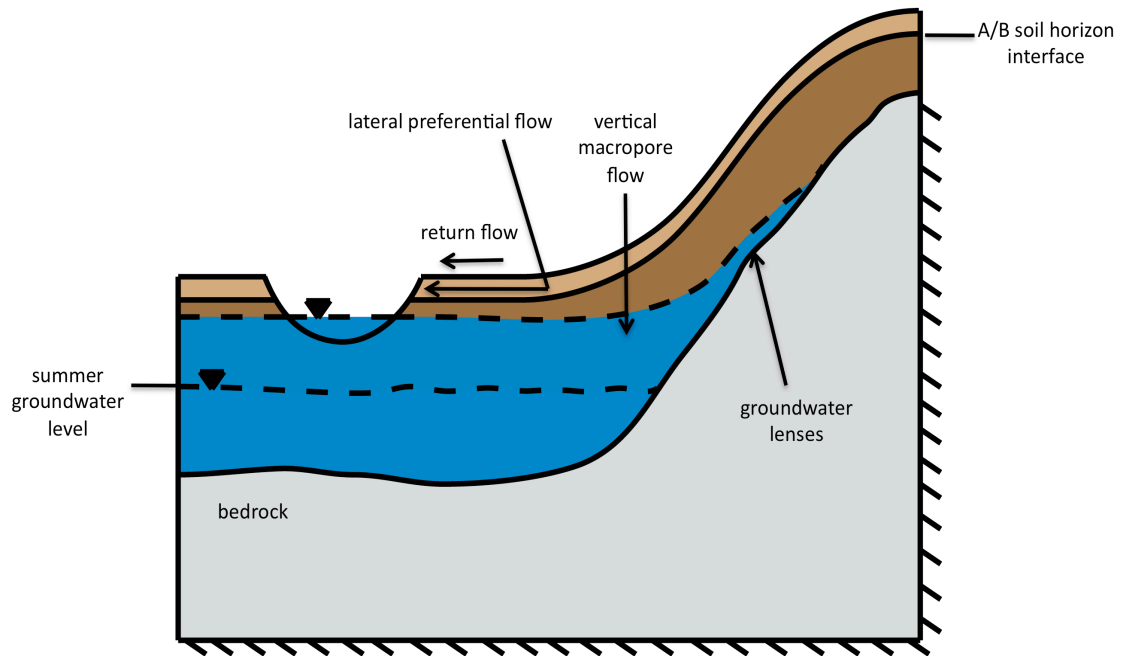


Figure 2-2. Theoretical cross-section of the Shale Hills catchment illustrating the conceptual flowpaths. The cross-section is not drawn to scale.

## Chapter 3

### $\delta^2\text{H}$ and $\delta^{18}\text{O}$ Results

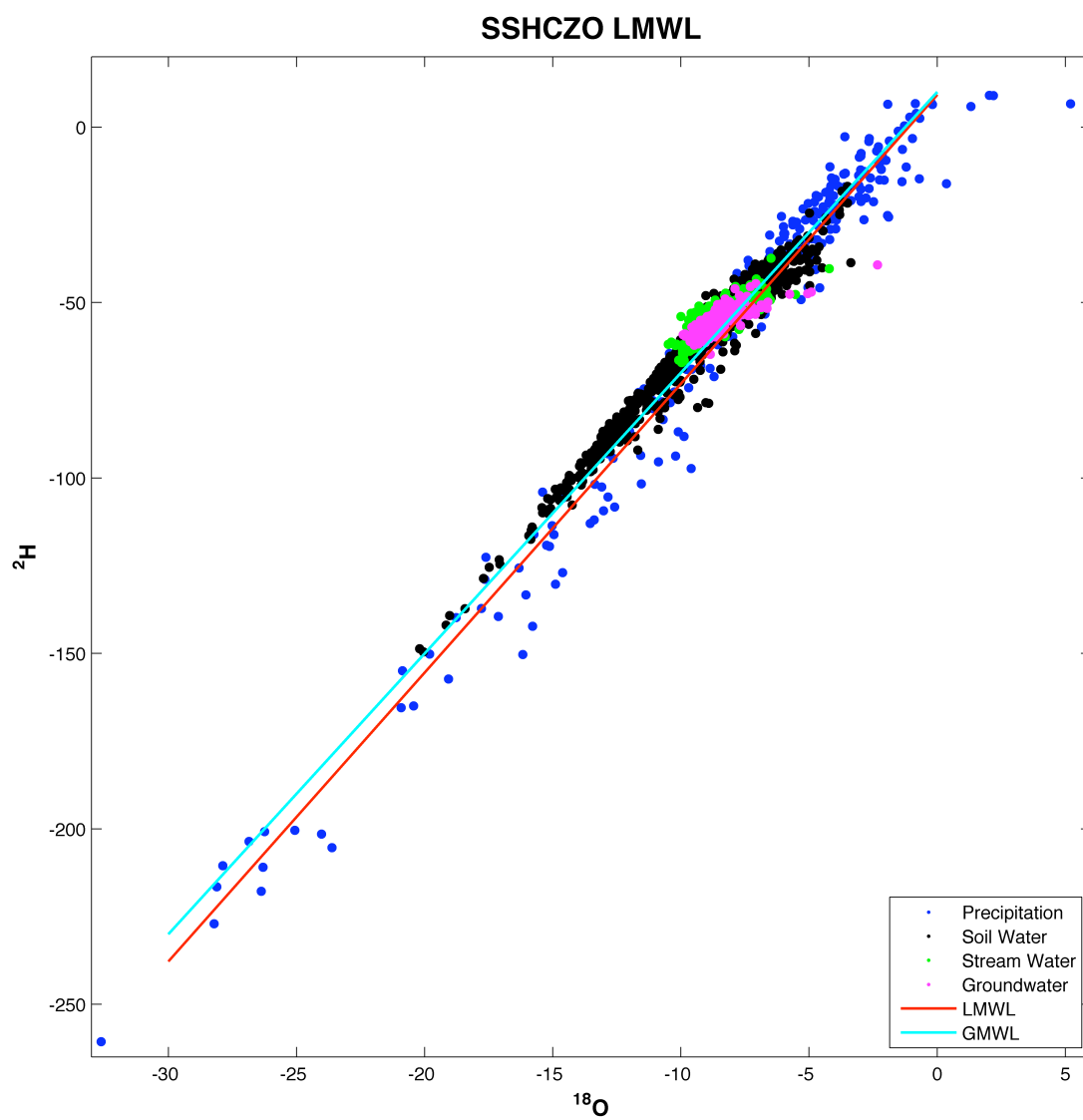
#### Meteoric Water Line

Water samples for  $\delta^2\text{H}$  and  $\delta^{18}\text{O}$  analysis have been collected at Shale Hills since 2008, currently totaling over 3000 samples. The lmwl plot for the Shale Hills  $\delta^2\text{H}$  and  $\delta^{18}\text{O}$  data is shown in Figure 3-1, and the averages for each pool in Table 3-1. The lmwl equation of the linear regression fit to the precipitation data is

$$\delta^2H = 8.24\delta^{18}O + 9.46$$

which is similar to gmwl equation and lmwl equations from this region of the US. The soil water, groundwater and stream water data mostly plot off of the lmwl, meaning that these pools undergo fractionation. The precipitation weighted average  $\delta^2\text{H}$  and  $\delta^{18}\text{O}$  is enriched relative to the other pools, which was also the conclusion of several other  $\delta^2\text{H}$  and  $\delta^{18}\text{O}$  studies from Central Pennsylvania (Deines et al., 1990; O'Driscoll et al., 2005). In general the soil water plots vary over a large range and are very similar to the precipitation. The groundwater and stream water have nearly identical  $\delta^2\text{H}$  and  $\delta^{18}\text{O}$  means, and while they plot in the same region their shapes are different. The difference in shape is better illustrated in Figure 3-1b, where the 95% quantile ellipse is plotted for each pool. The difference in size and slope of each pool signifies a difference in the variance and fractionation of the water in each pool. Therefore the groundwater has the lowest variance and is more fractionated than any other pool. The difference in statistical parameters between the pools suggests that the hydrology at the SSHCZO is complex, but knowing how the  $\delta^2\text{H}$  and  $\delta^{18}\text{O}$  is transformed in each pool will begin to unravel the relationships between the pools.

a.



b.

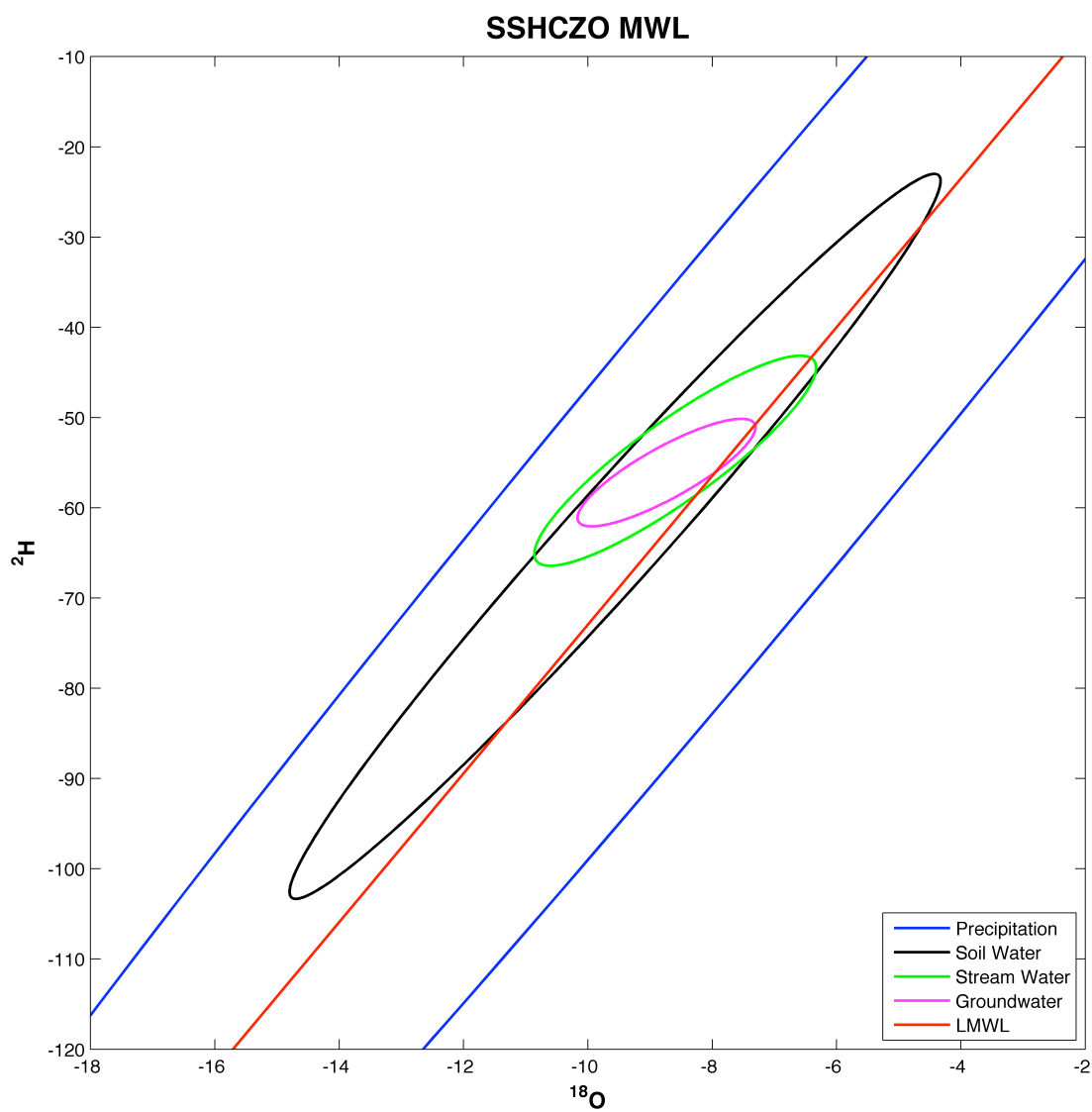


Figure 3-1: a. Local meteoric water line plot for the Shale Hills  $\delta^2\text{H}$  and  $\delta^{18}\text{O}$  data. The local (lmwl) and global (gmwl) meteoric water lines are both shown. b. Local meteoric water line plot using the 95% quantile ellipse for each pool. The quantile ellipses were calculated in Mathematica.

Table 3-1:  $\delta^2\text{H}$  and  $\delta^{18}\text{O}$  averages and other statistical parameters for the Shale Hills data. The precipitation average is weighted by the amount of precipitation.

	$\delta^2\text{H}$ Avg.	$\delta^{18}\text{O}$ Avg.	$\delta^2\text{H}$ Std Dev	$\delta^{18}\text{O}$ Std Dev	d- excess	Slope	Timeseries Samples (n)	Spatial Samples (m)
Precipitation	-52.22	-7.97	53.06	6.37	9.19	8.24	310	-
Soil Water	-57.91	-8.82	15.73	2.10	14.24	7.45	-	1190
Shallow Soil Water	-53.36	-8.04	17.99	2.38	12.94	7.32	-	308
Deep Soil Water	-63.15	-9.56	14.23	1.94	15.64	7.54	-	882
Groundwater	-56.09	-8.74	2.56	0.52	14.14	3.79	883	256
GW ISCO 1	-54.92	-8.58	1.90	0.54	13.93	2.69	631	-
GW ISCO 2	-59.04	-9.13	0.93	0.21	14.70	1.50	252	-
Stream Water	-54.78	-8.60	7.73	1.18	15.30	4.93	799	-

### Precipitation

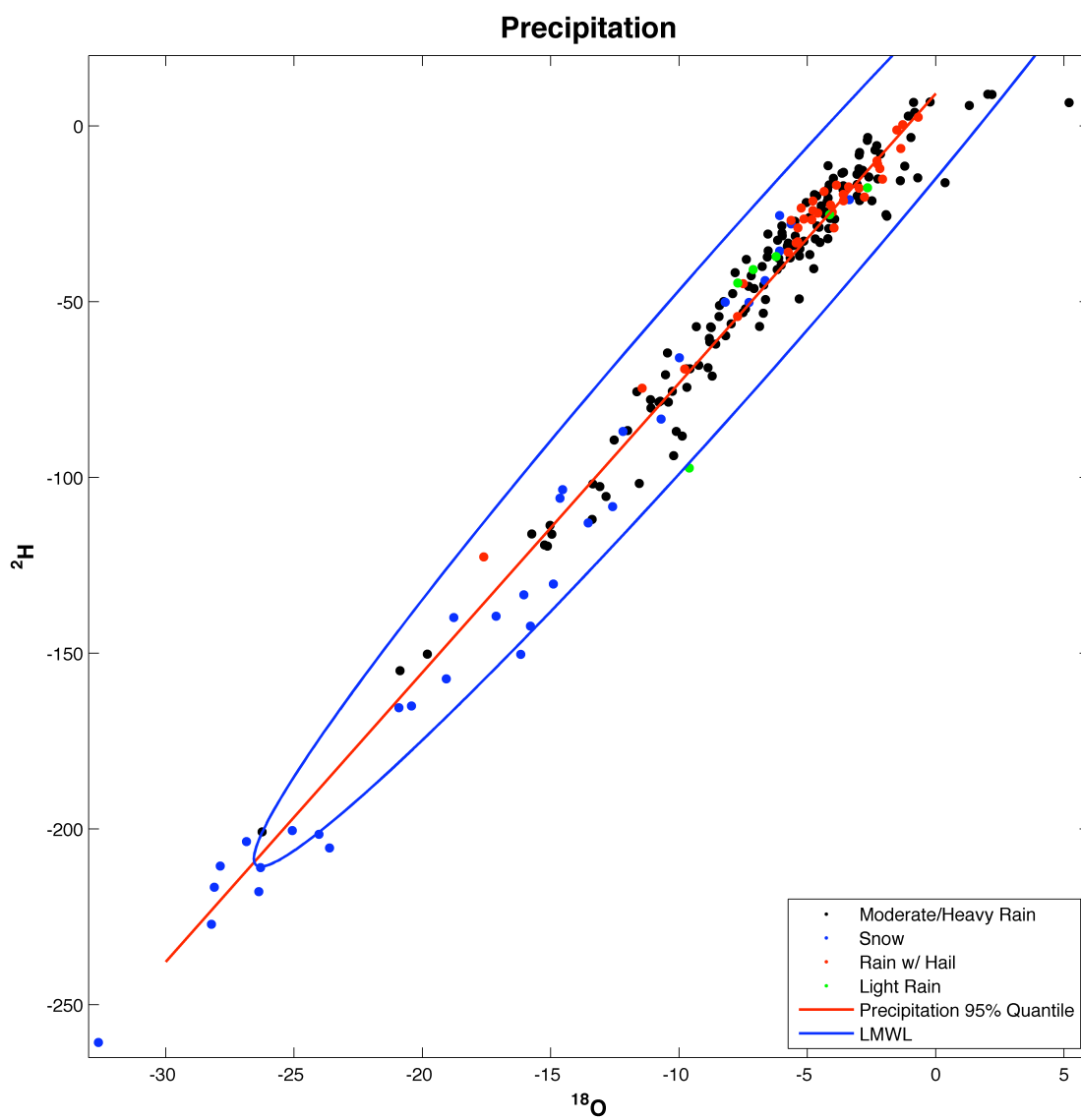
The Shale Hills catchment receives on average 995 mm of precipitation a year. Approximately 55% of precipitation falls during the growing season (April-September), with convective storms over the summer (June-September) and mostly snow over the winter (December-March). Precipitation is collected year-round and is assumed to be spatially consistent. In previous studies in Central Pennsylvania it was assumed that one rain gauge per 12.6km<sup>2</sup> was sufficient to resolve precipitation spatial variation (Reich, 1966; O'Driscoll et al., 2005).

The Eigenbrodt precipitation collector and lpm were both located at the weather station (Figure 2-1), which is an open area devoid of trees. Precipitation samples are not necessarily representative of the throughfall received by the catchment as a whole. The throughfall

precipitation spends time on the leaves and branches of the vegetation, evaporating to some extent before it reaches the soil surface. An experiment performed by DeWalle and Swistock (1994) in the same area of Central Pennsylvania showed that throughfall  $\delta^{18}\text{O}$  is enriched compared to precipitation collected at an open site. However the difference for  $\delta^{18}\text{O}$  averaged 0.2 - 0.3 ‰, which is the same as the precision of the DLT-100. Therefore it is assumed that throughfall  $\delta^2\text{H}$  and  $\delta^{18}\text{O}$  is the same as the sampled open area precipitation.

Precipitation has been sampled on an event basis since November 2008. The precipitation  $\delta^2\text{H}$  and  $\delta^{18}\text{O}$  data is shown in figure 3-2. Precipitation  $\delta^2\text{H}$  and  $\delta^{18}\text{O}$  has the largest variability relative to the other stores since it is a global process. The precipitation  $\delta^2\text{H}$  and  $\delta^{18}\text{O}$  is distinguished by plotting according to the precipitation type. The types used were snow, light rain/drizzle, moderate to heavy rain and rain containing hail. The most obvious distinction among the precipitation types is that the snow is depleted and the rain containing hail is enriched. The reason that the rain containing hail is enriched is because it occurs during convective storms over the summer. The warm temperatures lead to less fractionation and more water vapor replenishment by evapotranspiration. The light rain/drizzle contains evaporated samples because the atmosphere is sometimes not saturated during the event, causing evaporation of the droplets as they descend. The moderate to heavy rain shows a range of  $\delta^2\text{H}$  and  $\delta^{18}\text{O}$  because the events occur in any season and temperature. Storm path seems to have little control over the  $\delta^2\text{H}$  and  $\delta^{18}\text{O}$  of the event or the precipitation type. The seasonality of the precipitation isotope record is seen when plotting the monthly  $\delta^{18}\text{O}$  amount weighted time series. The precipitation is enriched over the summer and over the winter the precipitation is depleted due to cold temperatures.

a.



b.

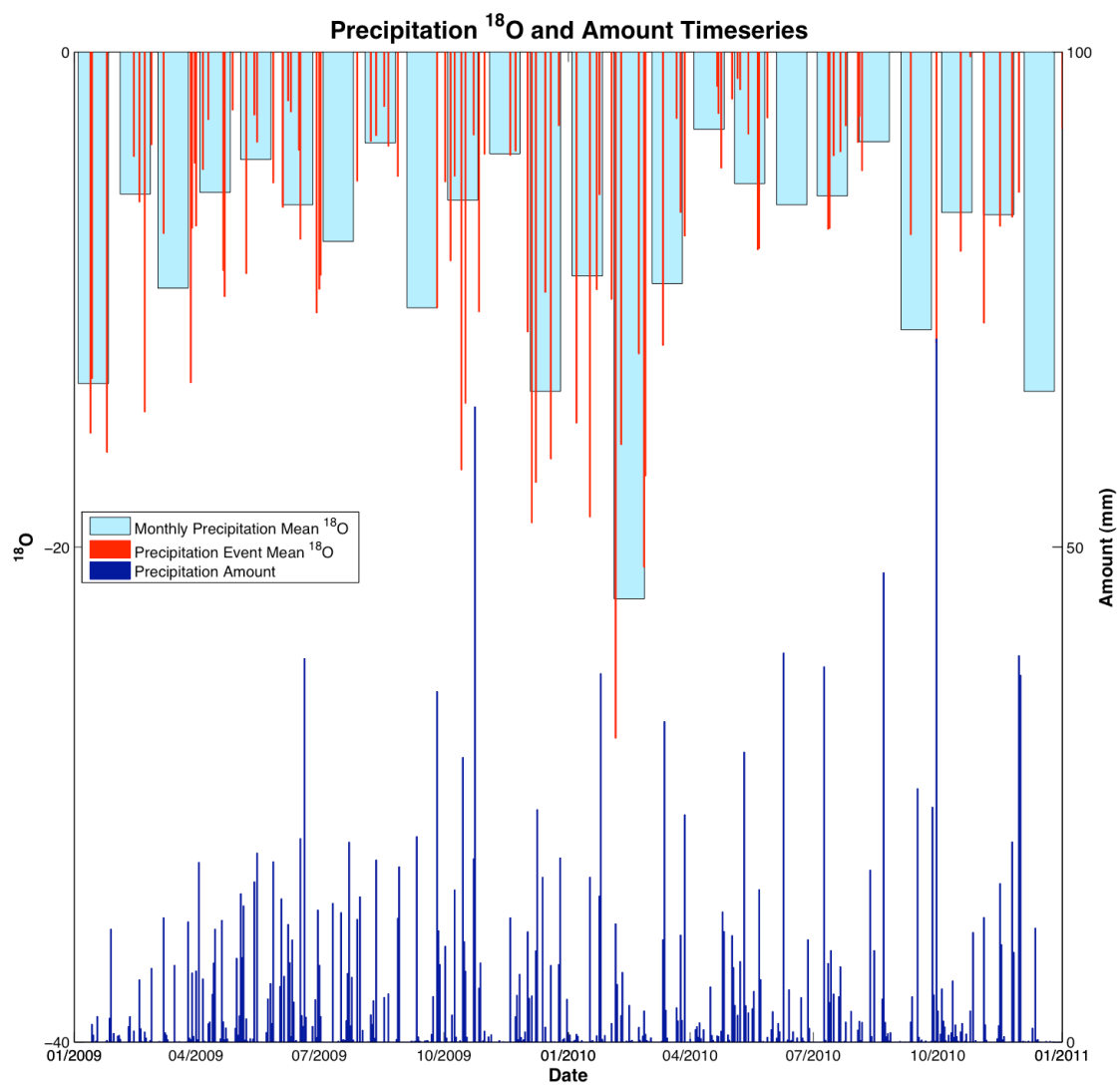


Figure 3-2: a. MWL plot showing the precipitation  $\delta^2\text{H}$  and  $\delta^{18}\text{O}$  grouped by precipitation type. The precipitation type was determined by the lpm. b. Time series of amount weighted event and monthly precipitation  $\delta^{18}\text{O}$  and the precipitation amount (mm).

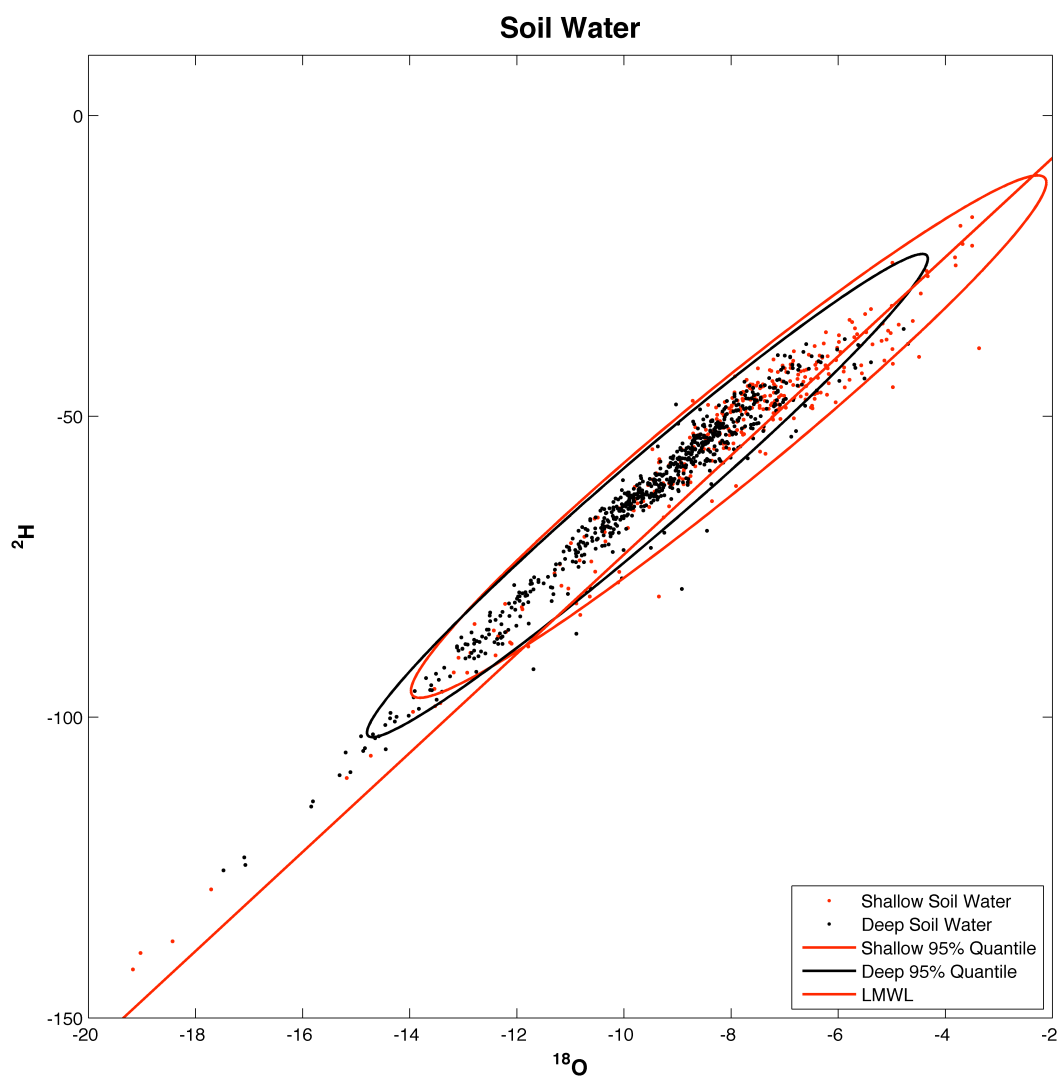
### Soil Water

Soil water is collected by the suction cup lysimeters (Soil Moisture 1900 series) at a vacuum of -0.5 bar. Soil water has been collected at Shale Hills since 06/13/2008 (Jin et al., 2011). The soil water  $\delta^2\text{H}$  and  $\delta^{18}\text{O}$  data is plotted on the lmwl in figure 3-3a. The soil water  $\delta^2\text{H}$  and  $\delta^{18}\text{O}$  data is separated into a shallow and deep group. The shallow group contains soil water samples collected from the top 30cm of the soil, and the deep group contains soil water samples from 40cm and below. The soil water is separated in this way because the A/B soil horizon interface is located at a depth of approximately 30cm, and this interface is less permeable and restricts the vertical infiltration of soil water (Lin et al., 2006). On average the shallow soil water is enriched compared to the deep soil water (Figure 3-3b). The enrichment is not the effect of evaporation, because the shallow soil water plots along the lmwl, not below the line where evaporated samples would plot. Instead the enrichment is the result of enriched summer precipitation only infiltrating the shallow soil. The amount weighted  $\delta^2\text{H}$  and  $\delta^{18}\text{O}$  of summer precipitation is -38.04‰ and -6.17‰ respectively. The soil water timeseries  $\delta^2\text{H}$  and  $\delta^{18}\text{O}$  shows a seasonal pattern that is similar to the precipitation. The deep soil water appears to have a  $\delta^{18}\text{O}$  composition that is more similar to the groundwater mean than the precipitation mean.

The linear regression of the soil water  $\delta^2\text{H}$  and  $\delta^{18}\text{O}$  data has a slope similar to that of the precipitation, although the soil water plots above the lmwl. This is where fractionated snowmelt would plot. This suggests that precipitation and snowmelt are infiltrating the soil most of the year.

Soil water is collected at different depths, different elevations, from the planar hill slope and swales and on the north and south slopes. The soil water  $\delta^2\text{H}$  and  $\delta^{18}\text{O}$  collected at different elevations (ridge-top, mid-slope and valley-floor) becomes more depleted down slope.

The different lysimeter transects have different  $\delta^2\text{H}$  and  $\delta^{18}\text{O}$  averages and variances based on their locations. The South Swale transect is depleted relative to the South Planar transect, and the North Planar transect is depleted relative to the South Planar transect. Overall the South and North Slopes have essentially the same average  $\delta^2\text{H}$  and  $\delta^{18}\text{O}$ , but the North Slope has a smaller variance.



a.

b.

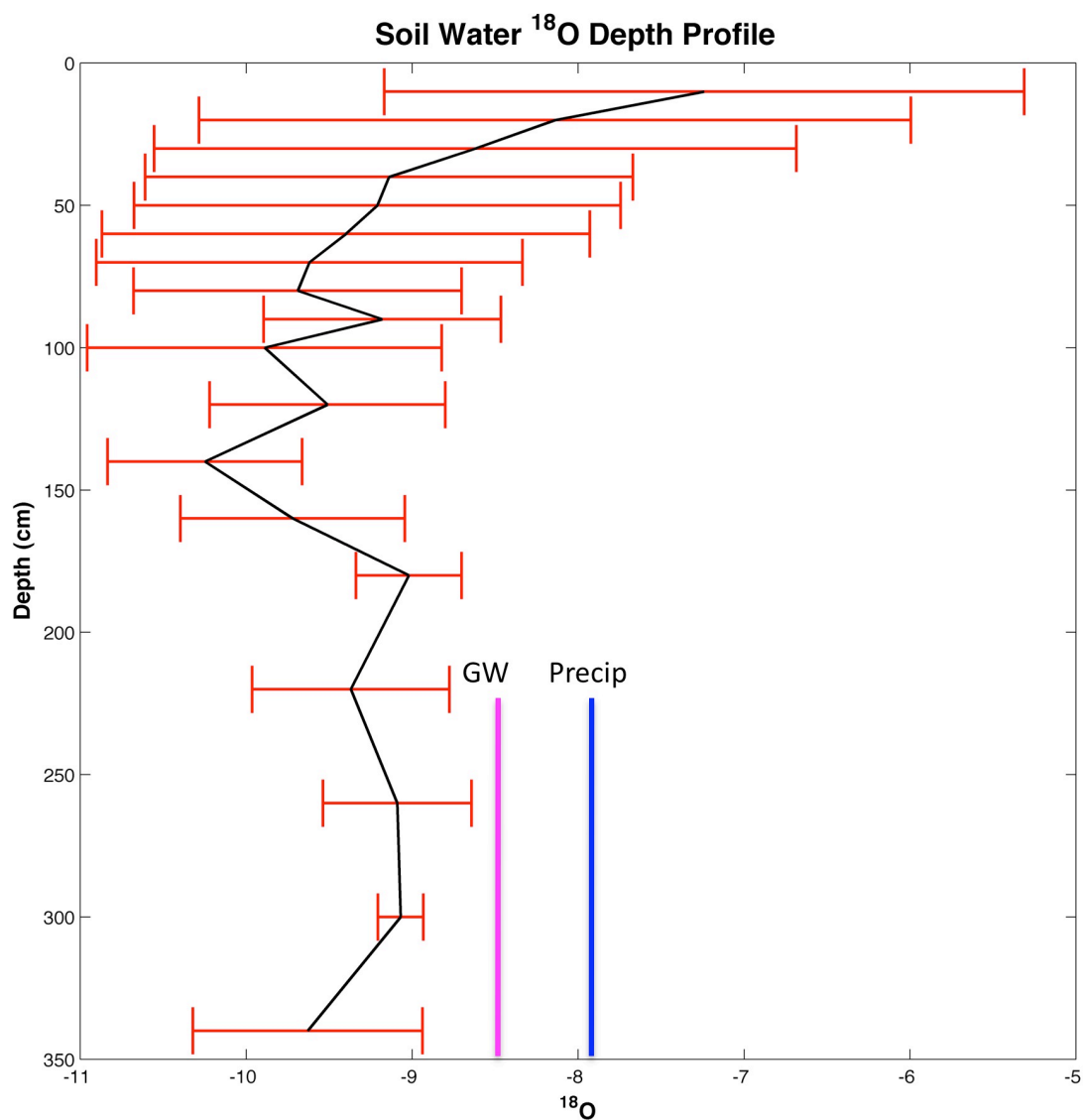
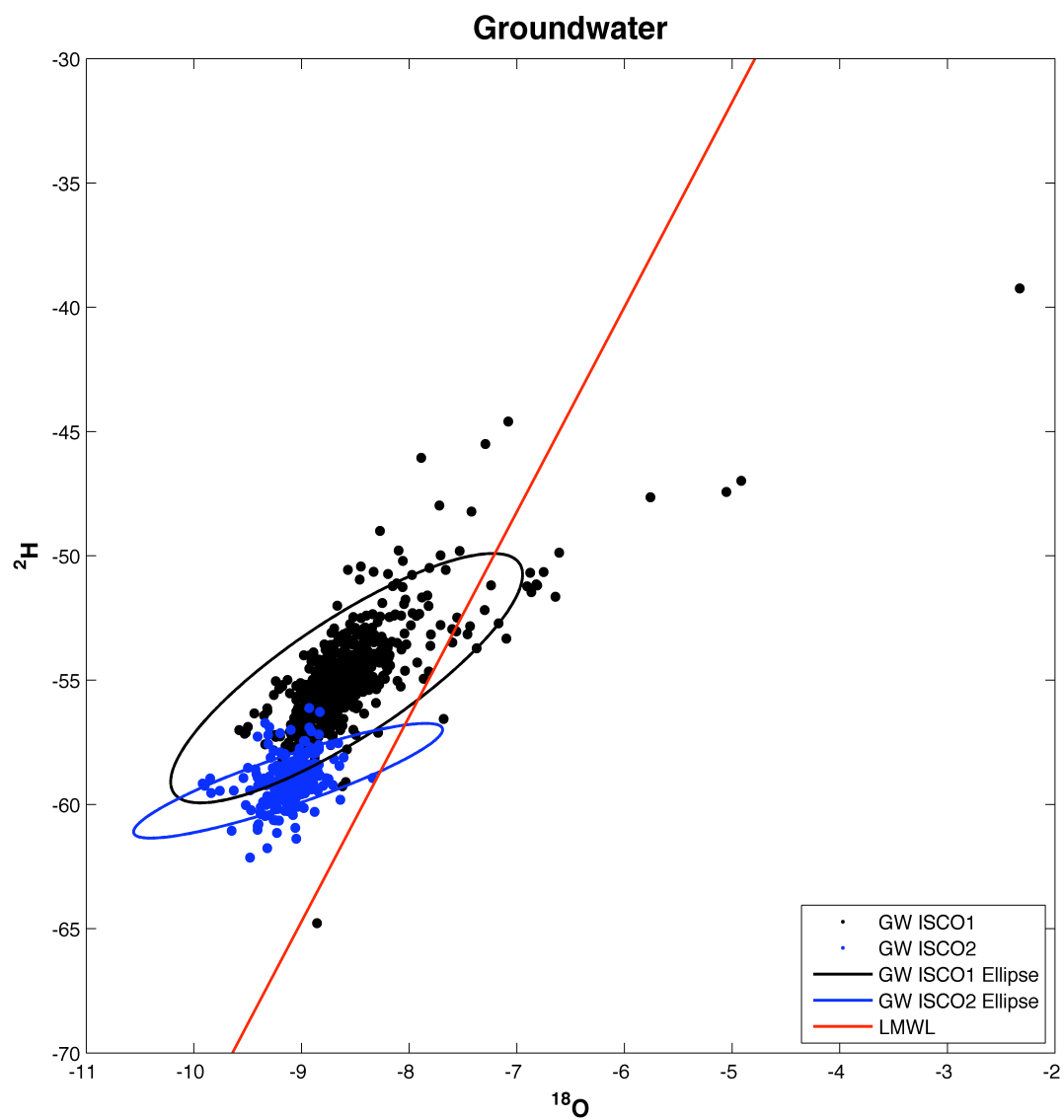


Figure 3-3: a. MWL plot of the soil water  $\delta^2\text{H}$  and  $\delta^{18}\text{O}$  grouped by depth region. b.. Average  $\delta^{18}\text{O}$  plotted by depth. The red lines are confidence intervals equal to  $\pm$  one standard deviation. The location of the groundwater and precipitation  $\delta^{18}\text{O}$  is shown for comparison.

## Groundwater

Groundwater is any saturated water located in the bedrock or soil and collected from the wells. Groundwater has been collected since 09/05/2008 at GW ISCO1 and since 02/25/2010 for GW ISCO2 at Shale Hills. The groundwater  $\delta^2\text{H}$  and  $\delta^{18}\text{O}$  data is plotted on the lmwl in figure 3-4a. The GW ISCO1 data are enriched relative to the GW ISCO 2 data. This suggests that as you move towards the outlet the groundwater becomes enriched, a pattern that is also seen in the groundwater data collected from wells 2-18. The groundwater  $\delta^2\text{H}$  and  $\delta^{18}\text{O}$  is consistent over time (Figure 3-4b), there is essentially no seasonality, but groundwater is significantly affected by fractionation. The majority of the groundwater isotopic signatures plot above the lmwl, which is where fractionated snowmelt plots. This would suggest that there is preference for cold season infiltration and recharge. This makes sense because the groundwater  $\delta^2\text{H}$  and  $\delta^{18}\text{O}$  mean is depleted relative to the precipitation mean. The points that plot to the right of the lmwl are evaporated samples. It appears that ISCO1 contains more evaporated samples than ISCO2. Although the groundwater depth fluctuates both seasonally and daily, the  $\delta^2\text{H}$  and  $\delta^{18}\text{O}$  is consistent at each location. This suggests that the groundwater has a long residence time, long enough to filter out the seasonal variations. Also, the changes in groundwater depth of up to 0.8m in a matter of days suggests that the groundwater is recharged rapidly.

a.



b.

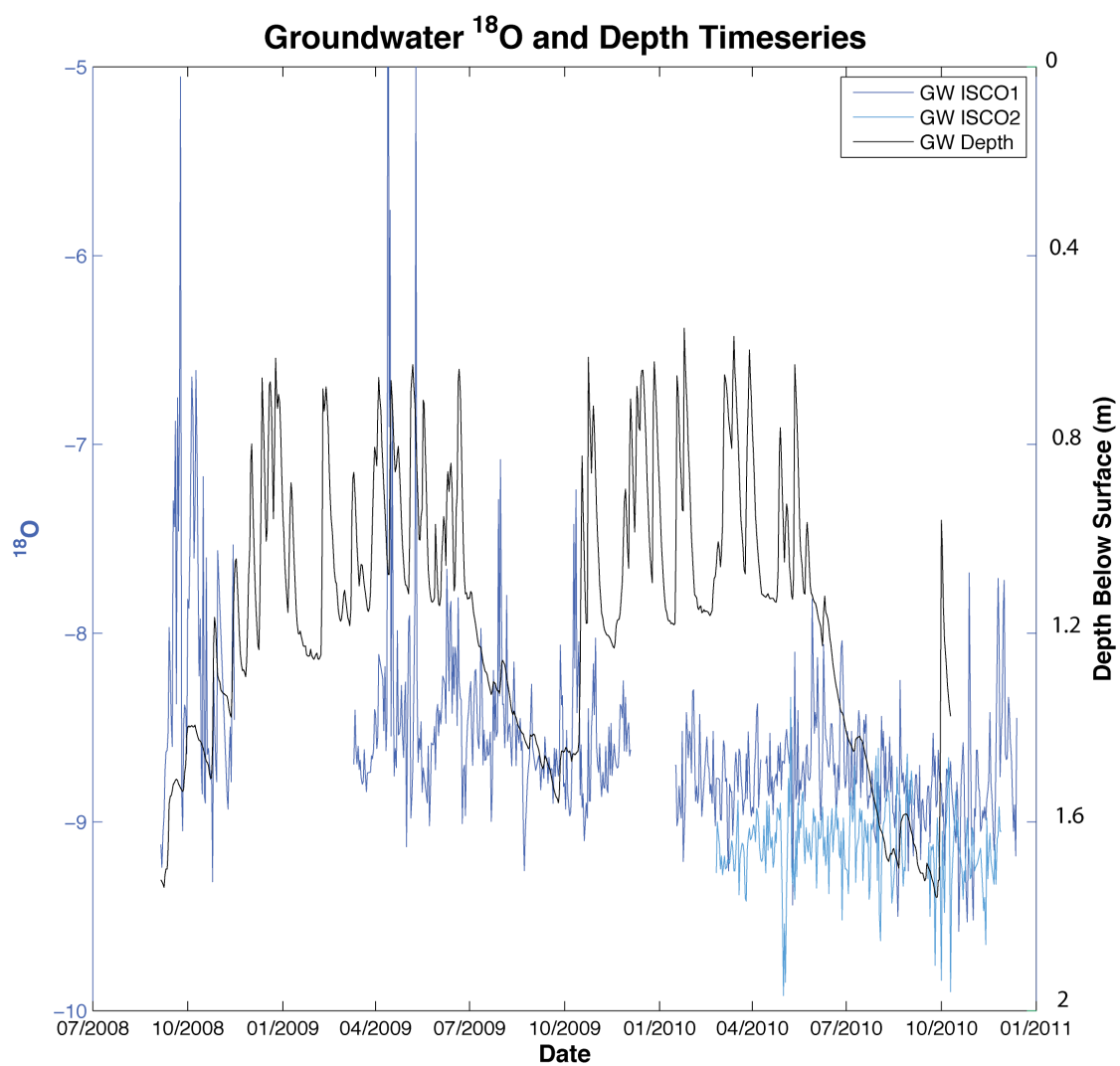
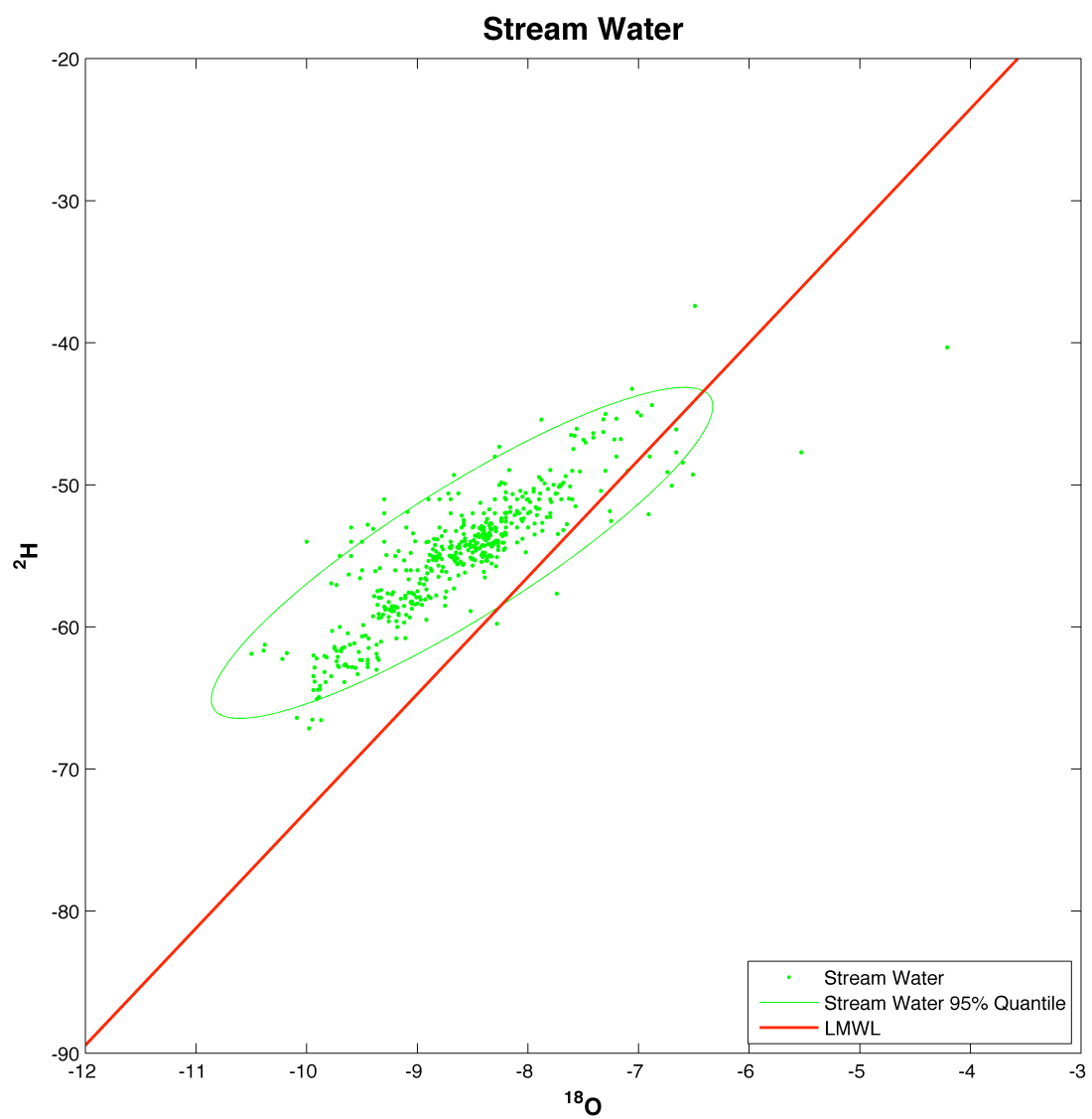


Figure 3-4: a. Local meteoric water line plot of the groundwater  $\delta^2\text{H}$  and  $\delta^{18}\text{O}$  data. b. Time series plot of the groundwater  $\delta^{18}\text{O}$  record and groundwater depth below the surface (m).

### Stream Water

Stream water has been collected daily since 03/28/2008 for  $\delta^2\text{H}$  and  $\delta^{18}\text{O}$  analysis. The streamwater  $\delta^2\text{H}$  and  $\delta^{18}\text{O}$  data is plotted on the lmwl in figure 3-5a. The average  $\delta^2\text{H}$  and  $\delta^{18}\text{O}$  is almost identical to groundwater, but the stream water variance and slope of the ellipse are higher. The low slope of the ellipse relative to the slope of the precipitation and soil water ellipses, is likely from fractionated source water rather than the water fractionating in the stream channel. The channel is short, approximately 200m long, and samples collected at upstream locations matched the samples collected at the outlet. The time series of stream water  $\delta^2\text{H}$  and  $\delta^{18}\text{O}$  along with discharge shows strong seasonality, like the precipitation and soil water, as well as significant daily/weekly changes, unlike the groundwater time series (Figure 3-5b). This suggests that the groundwater contributes to the stream water, but the increased variance and slope means that there are other contributors.

a.



b.

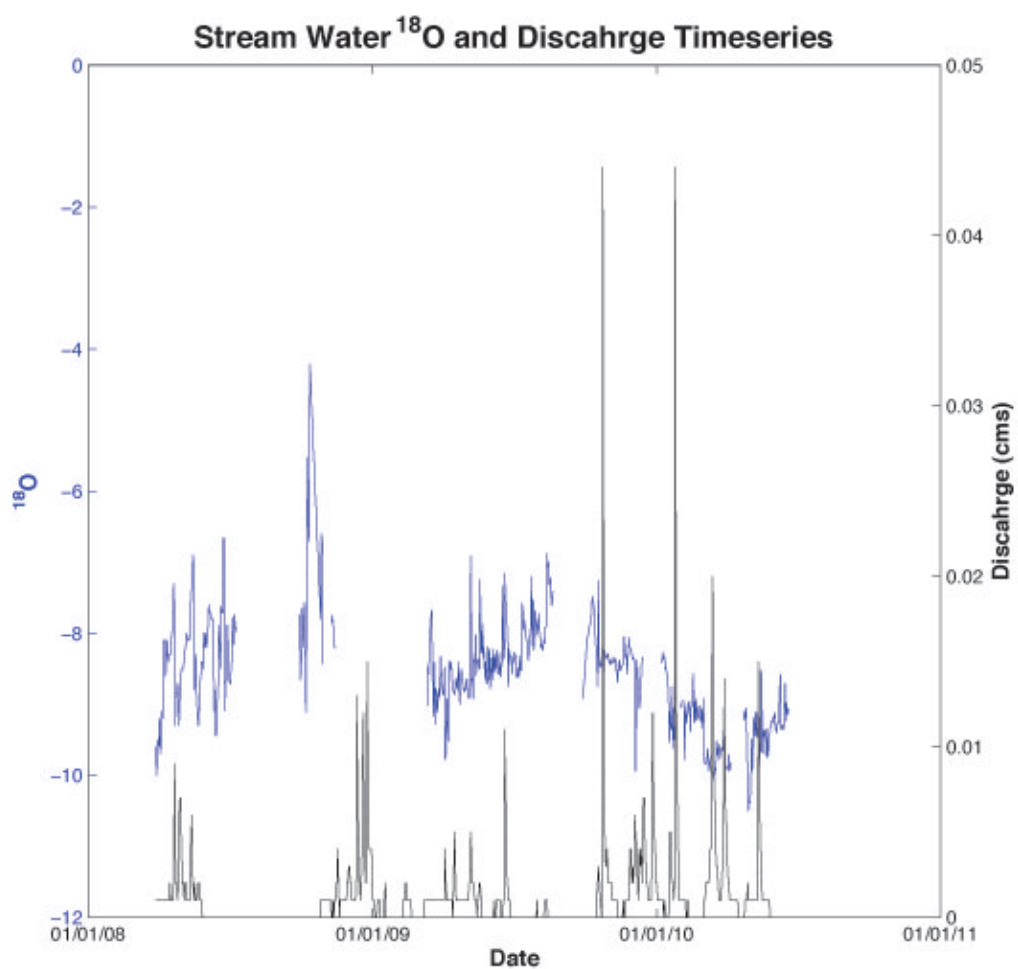


Figure 3-5: a. Local meteoric water line plot of the stream water  $\delta^2\text{H}$  and  $\delta^{18}\text{O}$  data. b. Time series plot of the stream water  $\delta^{18}\text{O}$  and the discharge ( $\text{m}^3/\text{s}$ ).

## Chapter 4

### $\delta^2\text{H}$ and $\delta^{18}\text{O}$ Discussion

Although several hydrologic studies have been performed at Shale Hills (Lynch, 1976; Duffy, 1996; Lin et al., 2006; Lin et al., 2008; Graham and Lin, 2011), there are a few things still unknown about the hydrologic functioning. These include the timing and composition of infiltration and recharge, how the soil water and groundwater interact, and the components of the stream water.

The difference in  $\delta^2\text{H}$  and  $\delta^{18}\text{O}$  between the precipitation, soil water and groundwater indicates that infiltration and recharge is selective. The mean  $\delta^2\text{H}$  and  $\delta^{18}\text{O}$  of the amount weighted precipitation is enriched relative to the soil water and groundwater mean. The summer precipitation is the most enriched, so this precipitation is not infiltrating past the shallow soil water. The precipitation from the rest of the year, late September to May, is infiltrating and recharging the soil water and groundwater. The mean  $\delta^2\text{H}$  and  $\delta^{18}\text{O}$  of the amount-weighted precipitation over the recharge period is -57.08‰ and -8.67‰ respectively. The overall soil water mean is nearly identical to the precipitation mean over this period, meaning that minimal infiltration occurs over the summer.

Regardless of how the precipitation  $\delta^2\text{H}$  and  $\delta^{18}\text{O}$  is averaged over the recharge period the weighted mean does not equal the mean of the overall groundwater or the ISCO1 and ISCO2 data. This indicates that groundwater recharge is not constantly occurring over the year but occurs during selective intervals. The explanation is that recharge occurs as mobile flow through macropores and preferential flowpaths during the non-growing season. Macropores and preferential flow paths are known to exist at Shale Hills (Lin et al., 2006; Lin, 2006; Lin and Zhou, 2008; Kuntz, 2010; Graham and Lin, 2011). It has been observed that preferential flow can

occur in the soils at Shale Hills as the matrix reaches a threshold moisture content. Beyond this threshold the isotopic signature of the macropore flow would not show up in the soil water (Graham and Lin, 2011). In the late stages of a precipitation event or after the vegetation water use stops in the fall season, precipitation continues to accumulate in the soil eventually activating the macropores. This explains why recharge occurs almost exclusively in the non-growing cool season and why the depleted isotopic signature of fall-winter-spring dominates the groundwater signature. During a precipitation event rainfall typically becomes more depleted over time due to the “amount” effect (Dansgaard, 1964). Therefore the water that composes the macropore flow is enriched relative to the water that will later saturate the soil. Furthermore we note that snowmelt comprises a large portion of the infiltration and recharge water in the non-growing season. Fractionation of snowmelt causes the data to plot above the lmwl due the difference in melting rates for  $\delta^2\text{H}$  and  $\delta^{18}\text{O}$  (Clark and Fritz, 1997). Selective infiltration and recharge, along with the preference for snowmelt water, explains why there is a difference between the  $\delta^2\text{H}$  and  $\delta^{18}\text{O}$  signatures of the precipitation, soil water and groundwater.

The  $\delta^2\text{H}$  and  $\delta^{18}\text{O}$  difference between the ISCO1 and ISCO2 groundwater is likely due to a difference in contributing area. In the back of the catchment there is essentially no contributing area. Since the vegetation uses a large portion of the soil water in the growing season, there is a large soil moisture deficit in this area. Consequently it will take more water to saturate the soil and initiate macropore flow to the groundwater. Therefore there is more of a preference for snowmelt recharge in this area, because snowmelt serves as a large pulse of water that is able to saturate the soil and reach the groundwater. After snowmelt occurs the groundwater samples from the wells in the back of the catchment become depleted, due to the depleted snowmelt water. As one moves to the front of the catchment there is more contributing area and thus the threshold to initiate macropore flow is slightly less than in the back of the catchment. A greater portion of

precipitation is then able to recharge the groundwater, which is enriched relative to the snowmelt. More research is needed to prove this hypothesis though.

Over the recharge period the water table is regularly fluctuating in the soil column (Figure 3-4b). As the groundwater moves through the soil it flushes the soil water and leaves behind its isotopic signature in the soil (Lynch and Corbett, 1989; Duffy, 1996). The deepest soil water samples from the South Slope have a mean  $\delta^2\text{H}$  and  $\delta^{18}\text{O}$  of -54.57‰ and -8.57‰ respectively, nearly identical to the GW ISCO 1 mean. The deepest soil water samples from the North Slope have a mean  $\delta^2\text{H}$  and  $\delta^{18}\text{O}$  of -61.97‰ and -9.61‰, respectively compared to a mean of -60.36‰ and -9.41‰ respectively for the three closest groundwater wells (9-11). The excursions of the water table tend to blend the groundwater isotope signatures through a simple flushing mechanism as proposed by Lynch and Corbett (1989) and Duffy and Cusumano (1996) for the Leading Ridge site based on  $\text{SO}_4$  data. It would appear though that the summer soil water is not flushed by the groundwater, which was the case at the Leading Ridge site. If this did occur then one would expect to see a pulse of enriched water enter the groundwater in the fall, which does not occur. This likely does not occur because evapotranspiration uses up so much soil water that any soil water remaining is in immobile pores that are not easily flushed.

The mean stream water  $\delta^2\text{H}$  and  $\delta^{18}\text{O}$  are nearly identical to the groundwater, and both pools plot in the same region on the Imwl (Figure 4-1), but the rotation and size of the quantile ellipses are dramatically different. Our interpretation is that the groundwater is the major contributor to the stream water, but that there is also water supplied by storage in the deeper soil matrix. Overland flow does occur at the valley floor, meaning that precipitation is contributing to the stream, but this only happens in large storms. The most plausible explanation is that soil water is also contributing to the stream water, with some portion being transported through preferential flowpaths. Preferential flowpaths exist in these soils, and figure 4-1 shows an example of a bubbling macropore adjacent to the stream after a large precipitation event.

Rotation and variance reduction of the quantile ellipse for the stream further shows that streamflow is a mix of the groundwater and soil water. We propose that stream flow is likely supplied by groundwater and the stormflow supplied by the soil water. Using a simple linear mixing model, which the long-term precipitation isotopic signature as the event water and the groundwater isotopic signature as the pre-event water, it was found that streamflow is 33% event water and 67% pre-event water. The mean  $\delta^2\text{H}$  and  $\delta^{18}\text{O}$  of the stream during baseflow is -54.71‰ and -8.61‰ respectively, and during non-baseflow -55.81‰ and -8.73‰ respectively. The baseflow mean is nearly identical to the GW ISCO1 mean, while the non-baseflow mean is more depleted, due to the contributions from soil water.



Figure 4-1: Picture of a preferential flowpath emptying directly into the stream from the North bank at the SSHCZO.

## Chapter 5

### Age Model

#### Derivation

An age model was derived for piecewise constant inputs based on Duffy and Cusumano (1998) and Duffy (2010). The purpose of the model is to begin to establish a theoretical basis for the conceptual model described in previous sections, and to evaluate the likely mean age of the water at Shale Hills from the stable isotope signatures. The equations for the flow and concentration are from Duffy and Cusumano (1998). Their model describes the concentration-discharge dynamics in a small watershed dominated by subsurface storage. The flow is assumed to be of the form  $Q = k(V - V_s)$ , where  $k$  is a rate constant and  $V_s$  is the residual storage volume. The piece-wise constant input equations for the flow and concentration are:

$$Q_{j+1} = Q_j e^{-k\Delta t} + Q_{i,j+1} (1 - e^{-k\Delta t})$$

$$C_{j+1} = C_j G_{j+1} + C_{i,j+1} (1 - G_{j+1})$$

$$G_{j+1} = \left( \frac{Q_{i,j+1} - Q_{j+1}}{Q_{i,j+1} - Q_j} \cdot \frac{Q_j + kV_s}{Q_{j+1} + kV_s} \right)^{\frac{Q_{i,j+1}}{R(Q_{i,j+1} + kV_s)}}$$

where  $Q$  is the streamflow,  $Q_i$  is the input to the catchment,  $C$  is the streamflow concentration,  $C_i$  is the input concentration,  $R$  is the retardation coefficient,  $j$  is the time step and  $\Delta t$  is the time step length. The reader is referred to Duffy and Cusumano (1998) for details. The theoretical rate constant  $k$  and the residual storage volume  $V_s$  can be estimated from the data. By plotting

discharge vs storage volume,  $k$  is the slope of the line fit to the data and  $V_s$  is the volume when there is zero discharge.

The age concentration equation is derived by explicitly solving for the age concentration from Duffy (2010). The piece-wise constant input age concentration equation is:

$$\alpha_{j+1} = C_{j+1} + \alpha_j \left(1 - \frac{Q_{i,j+1}}{V_{j+1}} \Delta t\right)$$

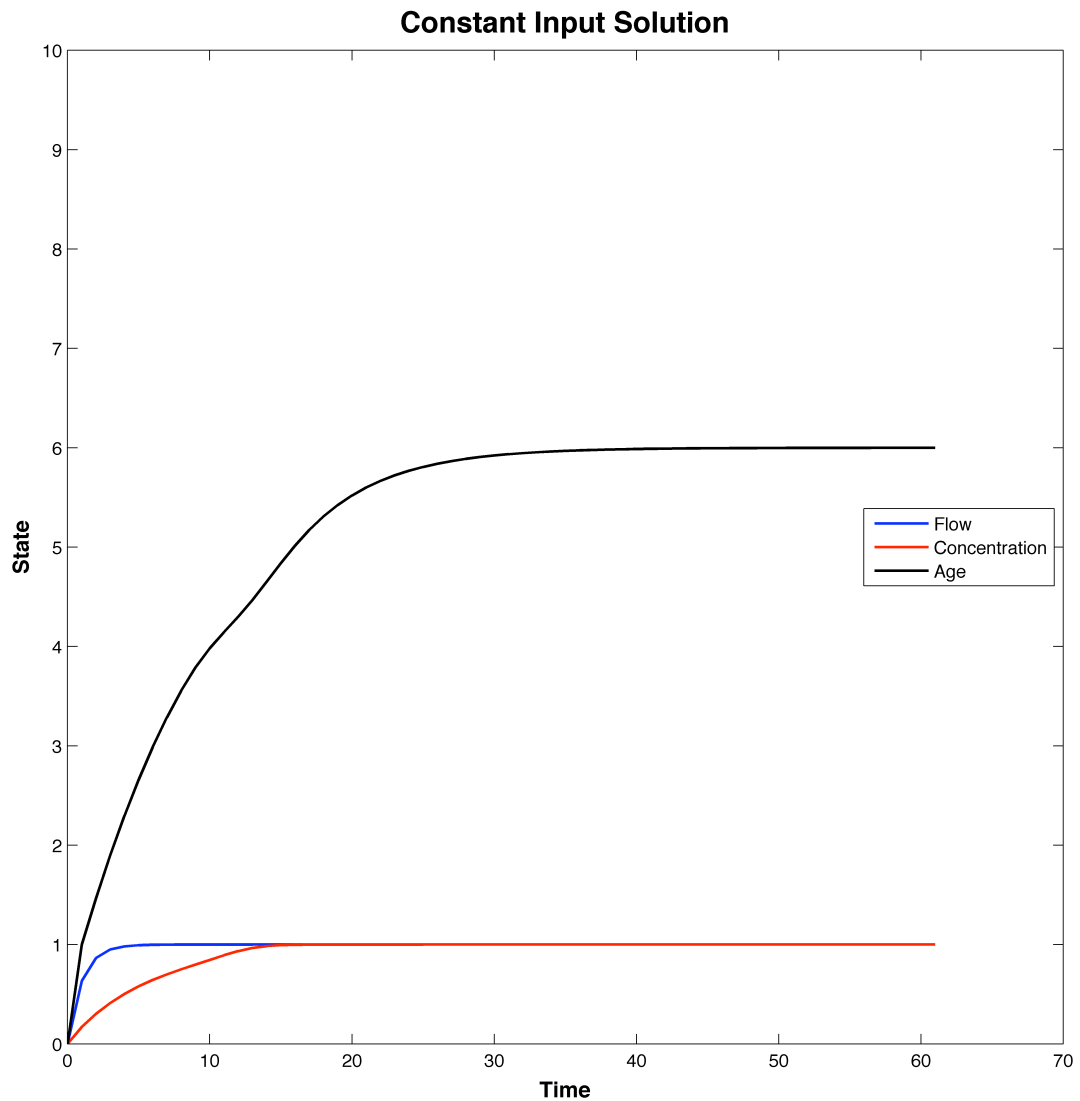
where  $\alpha$  has units of  $MT/L^3$ . The mean age is (Duffy, 2010)

$$A_{j+1} = \frac{\alpha_{j+1}}{C_{j+1}}$$

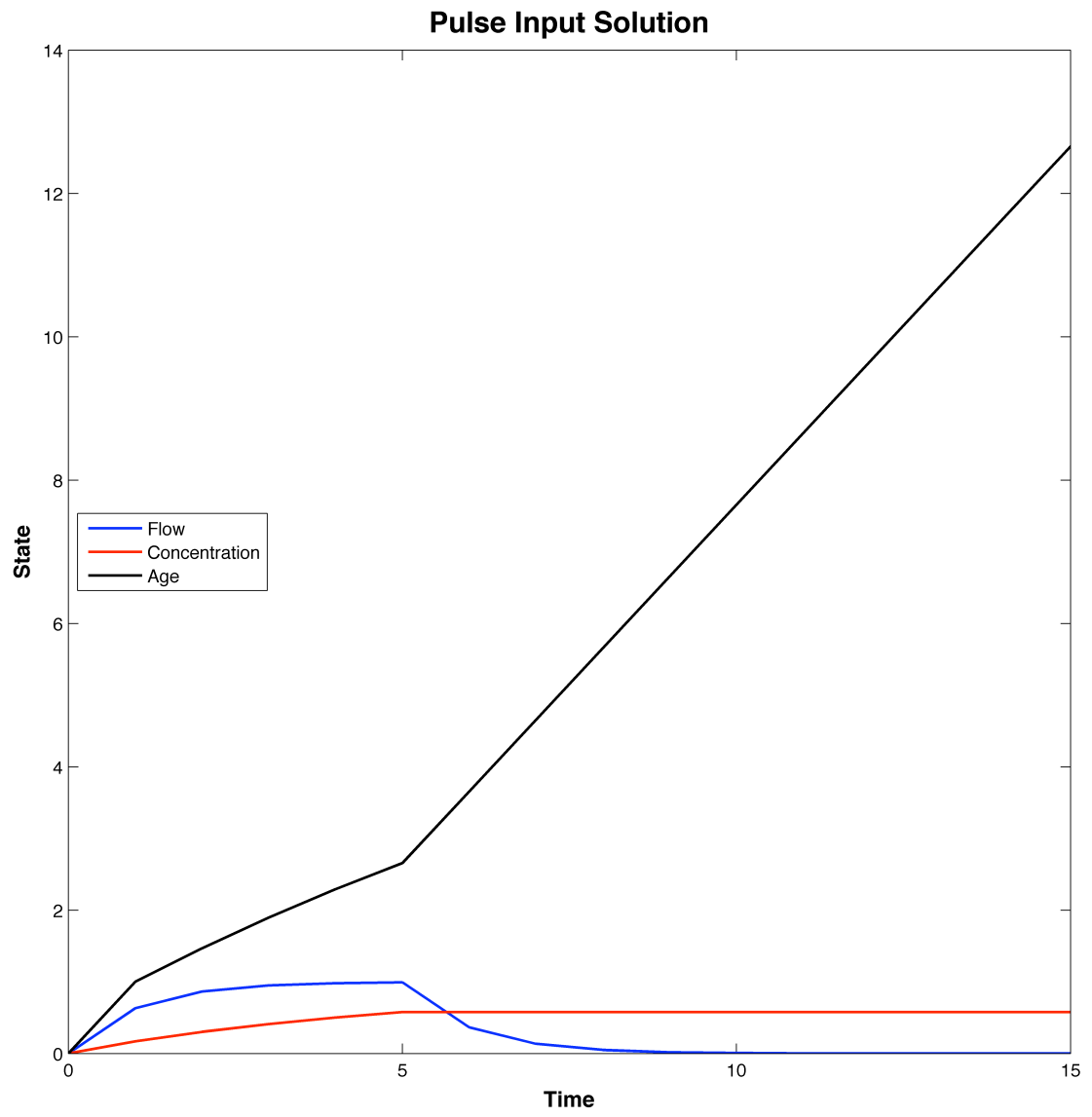
where the units of the age are time.

The age model was tested against an analytic solution from Duffy (2010) for the constant input case (Figure 5-1a). The inputs were chosen arbitrarily as  $Q_i = C_i = k = 1$ ,  $V_s = 5$  and  $\Delta t = 1$ , and the initial conditions are  $Q(0) = C(0) = A(0) = 0$ . The age found by the analytic equation and the age model is 5.999727. The age model was further tested by using a pulse input and an oscillating input scenario (Figure 5-1b/c). For the pulse input  $Q_i = C_i = 1$ , ( $0 < t \leq 4$ ) and  $= 0$  for  $t > 4$ . The rest of the parameters and the initial conditions were the same. Once the recharge stops the system begins to age linearly, since there is no water being added that has an age of zero. Therefore the water in the system is aging by a factor of one with each time step until it is removed from the system by streamflow. This can be thought of as aging like a clock, with each increase in clock time the age of the water increases by the same amount. For the oscillating input scenario  $Q_i$  and  $C_i$  alter between values of 1 and 0 every 4 time steps. For this case the age

of the system increases linearly when there is no recharge and then decreases when there is recharge of zero age being added to the system. As the system reaches steady state the age oscillates around an approximate value of 11, which is equal to the steady state residence time calculated as  $V/Q$ . These three test cases verify the accuracy of the age model, which will now be used to determine the mean age of the water exiting the SSHCZO.



a.



b.

c.

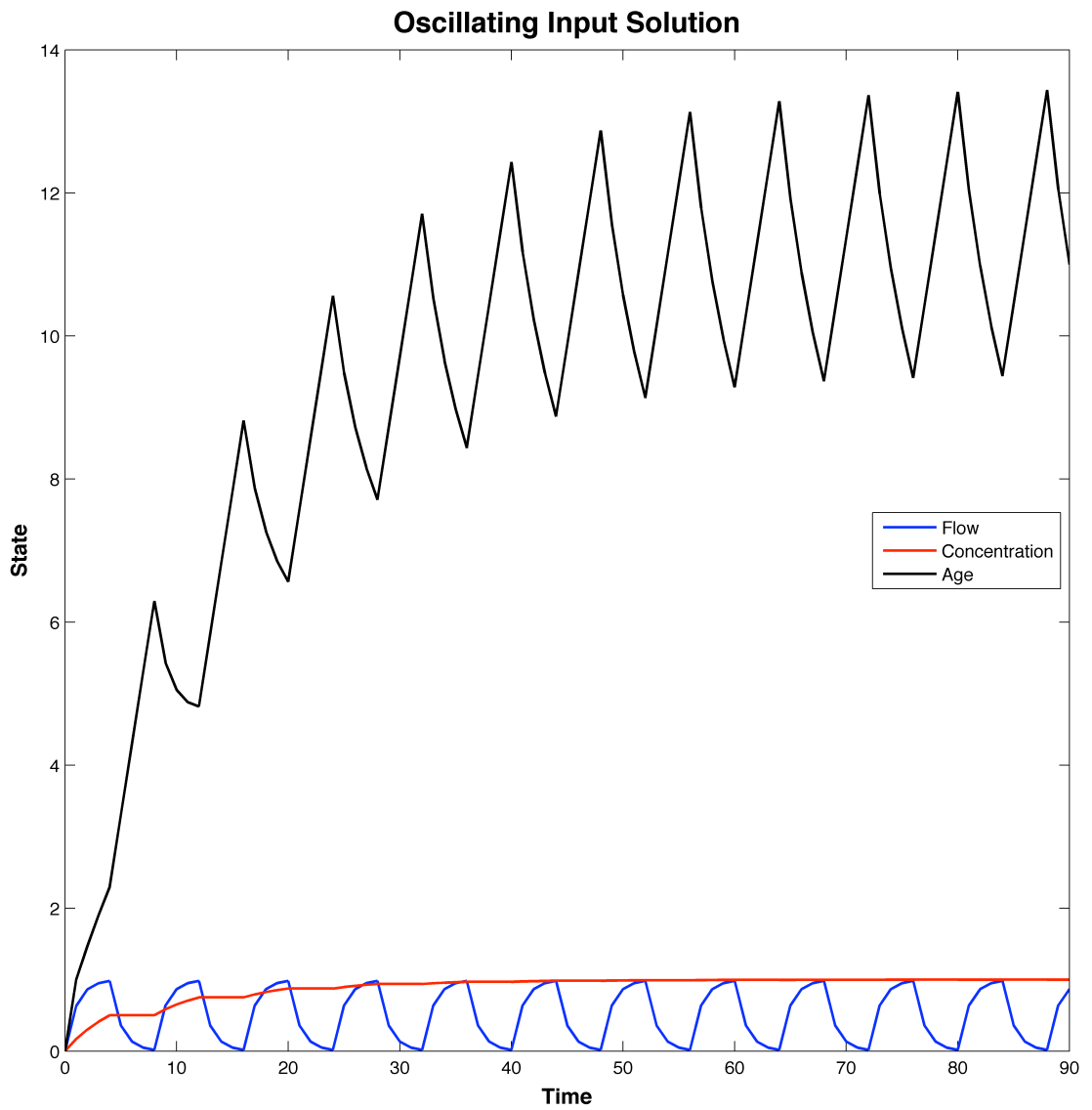


Figure 5-1. a. The solution to the piecewise constant inputs age model, for the case of a constant input. b. The solution to the piecewise constant inputs age model for the case of a pulse input. c. The solution to the piecewise constant inputs age model for the case of an oscillating input.

### Age Model Results and Discussion

The age model for the SSHCZO was run using a monthly time step for January 2009 – December 2010. This period was chosen because it had the most complete isotopic and hydrologic data record.  $Q_i$  was the monthly groundwater recharge, calculated using the PIHM model (Qu and Duffy, 2007). PIHM is a fully coupled multi-process hydrologic model. The PIHM model was run using 32 years of forcing data (1979 – 2010), and was calibrated by Xuan Yu (unpublished). The recharge input was chosen over the precipitation because there are periods, summer and parts of the winter, where the majority of the precipitation does not recharge either because of large soil moisture deficits or frozen soil.  $k$  was estimated from the data plotted in figure 5-2 to be 1.64 and  $V_s$  was 17443.06 m<sup>3</sup>. The discharge and volume data were monthly means from 2009 and 2010, and they also came from PIHM. This data was chosen over the field data because there was no easy way to accurately calculate the storage volume and thus the field data was noisy.  $C_i$  was the amount weighted mean precipitation  $\delta^2\text{H}$  and  $\delta^{18}\text{O}$ . The initial condition for  $Q$  was the flow for December 2008, and for  $C$  the concentration from March 2009. The age of the recharge input was assumed to be zero, but the initial age of the water in the catchment was not zero. The initial age was 6 months, which was estimated from the long-term average  $V/Q$ . The data used in the age model is given in Table 5-1.

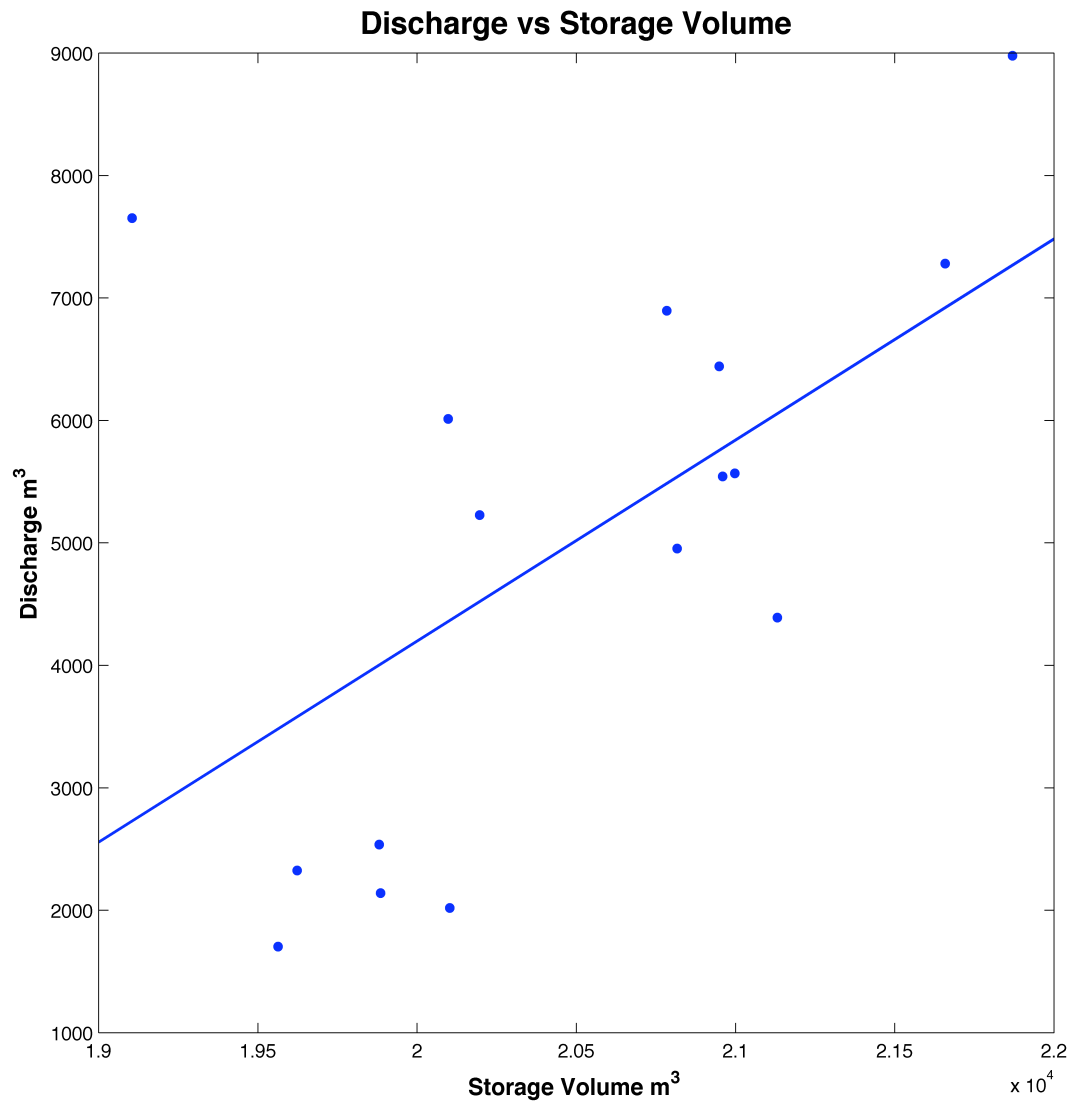


Figure 5-2. The discharge-volume relationship for the Shale Hills data. The discharge and volume data come from the PIHM model (Qu and Duffy, 2007), which was run using 32 years of forcing data. The data plotted are monthly means from 2009 and 2010.

Table 5-1. The monthly mean data used for the piecewise constant inputs age model for the SSHCZO

Month	Streamflow (m <sup>3</sup> /month)	Infiltration (m <sup>3</sup> /month)	Precipitation $\delta^2\text{H}$	Precipitation $\delta^{18}\text{O}$	Streamflow $\delta^2\text{H}$	Streamflow $\delta^{18}\text{O}$
Dec 2008	10830.65	7843.55				
Jan 2009	912.32	955.04	-114.07	-13.39		
Feb 2009	1245.60	1748.47	-34.08	-5.74		
Mar 2009	1930.52	1746.38	-64.34	-9.54	-54.13	-8.59
Apr 2009	3461.78	2989.01	-30.40	-5.67	-55.55	-8.82
May 2009	3242.04	4332.11	-24.03	-4.34	-54.83	-8.40
Jun 2009	3034.28	3178.75	-37.13	-6.17	-53.37	-8.29
Jul 2009	451.65	4095.09	-53.82	-7.65	-51.84	-8.11
Aug 2009	658.29	0.00	-18.13	-3.67	-48.53	-7.64
Sep	27.97	1975.39	-64.23	-10.33	-51.27	-8.24

2009						
Oct						
2009	7193.60	8280.48	-33.28	-5.98	-52.76	-8.21
Nov						
2009	2825.67	1369.70	-16.39	-4.11	-53.51	-8.37
Dec						
2009	10109.25	6064.71	-101.53	-13.71	-55.91	-8.71
Jan201						
0	9493.97	4730.58	-61.62	-9.05	-57.05	-8.92
Feb						
2010	908.22	1271.63	-173.33	-22.09	-58.15	-9.08
Mar						
2010	11769.96	6200.69	-64.98	-9.35	-62.58	-9.71
Apr						
2010	2595.07	783.57	-19.04	-3.12	-60.97	-9.48
May						
2010	4799.66	3746.13	-32.73	-5.31	-61.33	-9.49
Jun						
2010	200.22	0.00	-37.13	-6.17	-58.06	-9.15
Jul						
2010	12.70	0.00	-38.23	-5.81		
Aug						
2010	1.91	0.00	-21.84	-3.62		

Sep						
2010	0.00	7783.13	-80.52	-11.22		
Oct						
2010	0.00	1341.74	-41.87	-6.48		
Nov						
2010	0.00	7708.45	-35.79	-6.57		
Dec						
2010	0.00	2784.92	-101.53	-13.71		

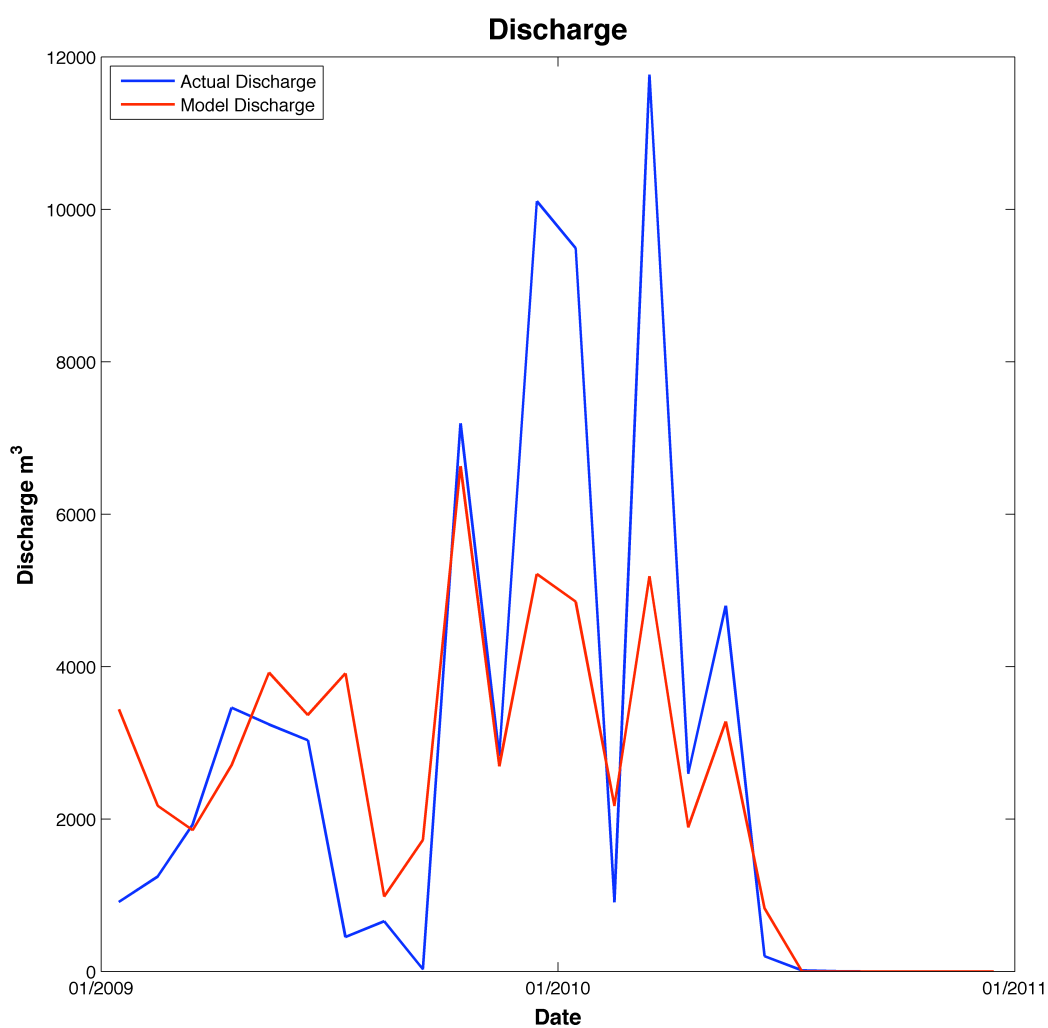
The solution to the flow equation and concentration equation is shown in figure 5-3, plotted with the actual flow and concentration. There was an additional constraint on the flow equation, which was when  $V < V_s$ ,  $Q=0$ . In this case the volume was estimated from the measured stream stage data as  $V = \text{stage} * \text{area} * \text{porosity}$ , where the area was  $80127.757 \text{m}^2$  and the porosity was 0.33. This additional condition was necessary because the flow equation always assumed that  $V_s$  was full and therefore all of the recharge was initiating streamflow. Overall the modeled flow follows the same pattern as the measured flow. The concentration was modeled using  $R = 1.5$ , which was chosen because it increased the accuracy of the model. The increase in concentration in November 2010 was likely due to an unusually enriched precipitation  $\delta^2\text{H}$  and  $\delta^{18}\text{O}$  during that month. Overall the modeled concentration follows the pattern of the measured concentration.

The mean age of the Shale Hills water is shown in figure 5-3c. The age fluctuates between 4 and 9 months, with an overall mean age of approximately 5-6 months for the catchment. During times of high flow the age decreases and during times of low flow the age

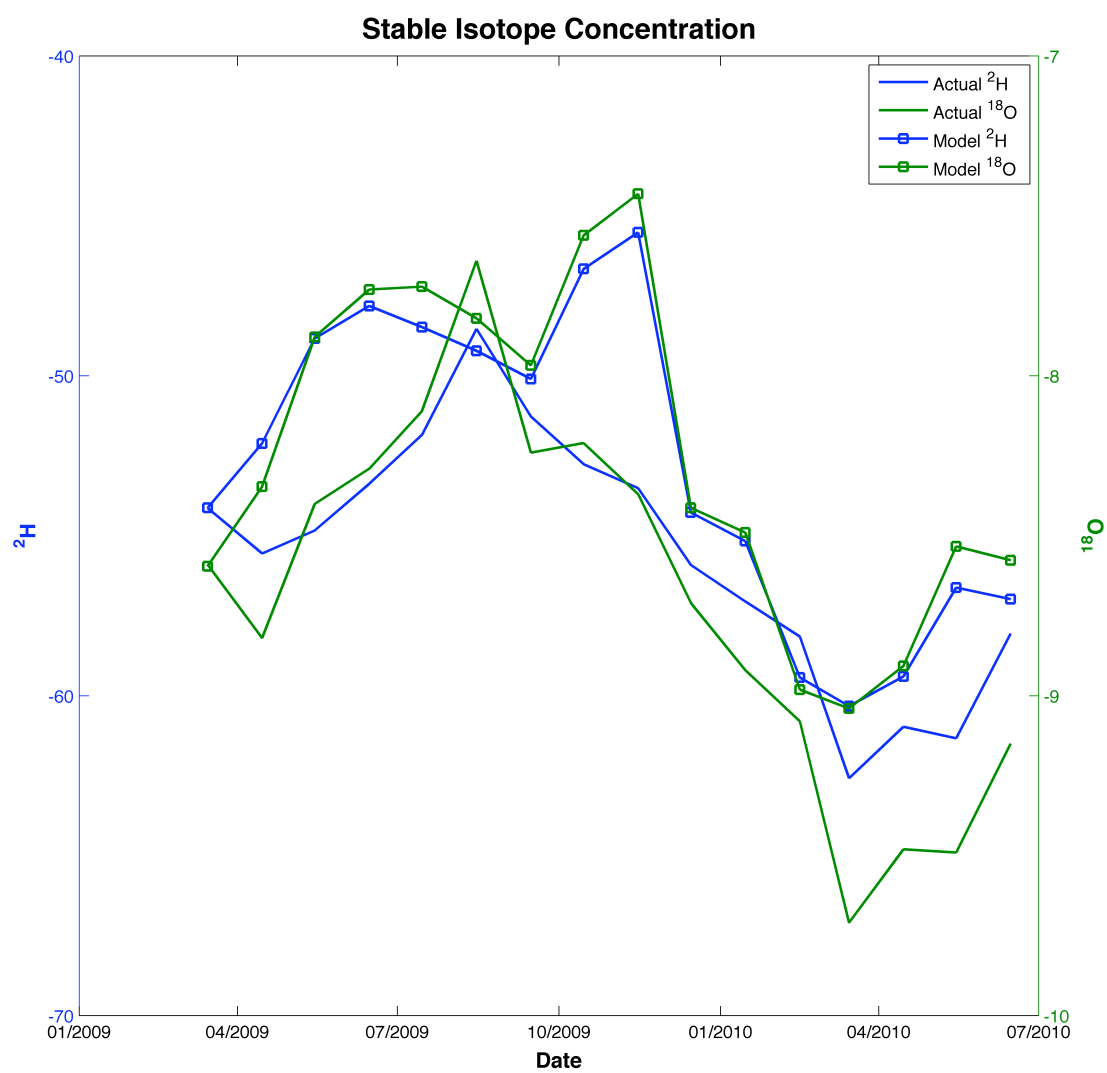
increases almost linearly. Although there is no flow for the period of July 2010 – December 2010, the age actually decreases because there is recharge occurring that has an age of zero.

The ages of the soil water and groundwater are probably different than the age of the water from the entire catchment. The groundwater is likely older than 6 months, which would explain why the seasonality is filtered out. The soil water is probably younger than 6 months since the soil water is similar to precipitation.

a.



b.



c.

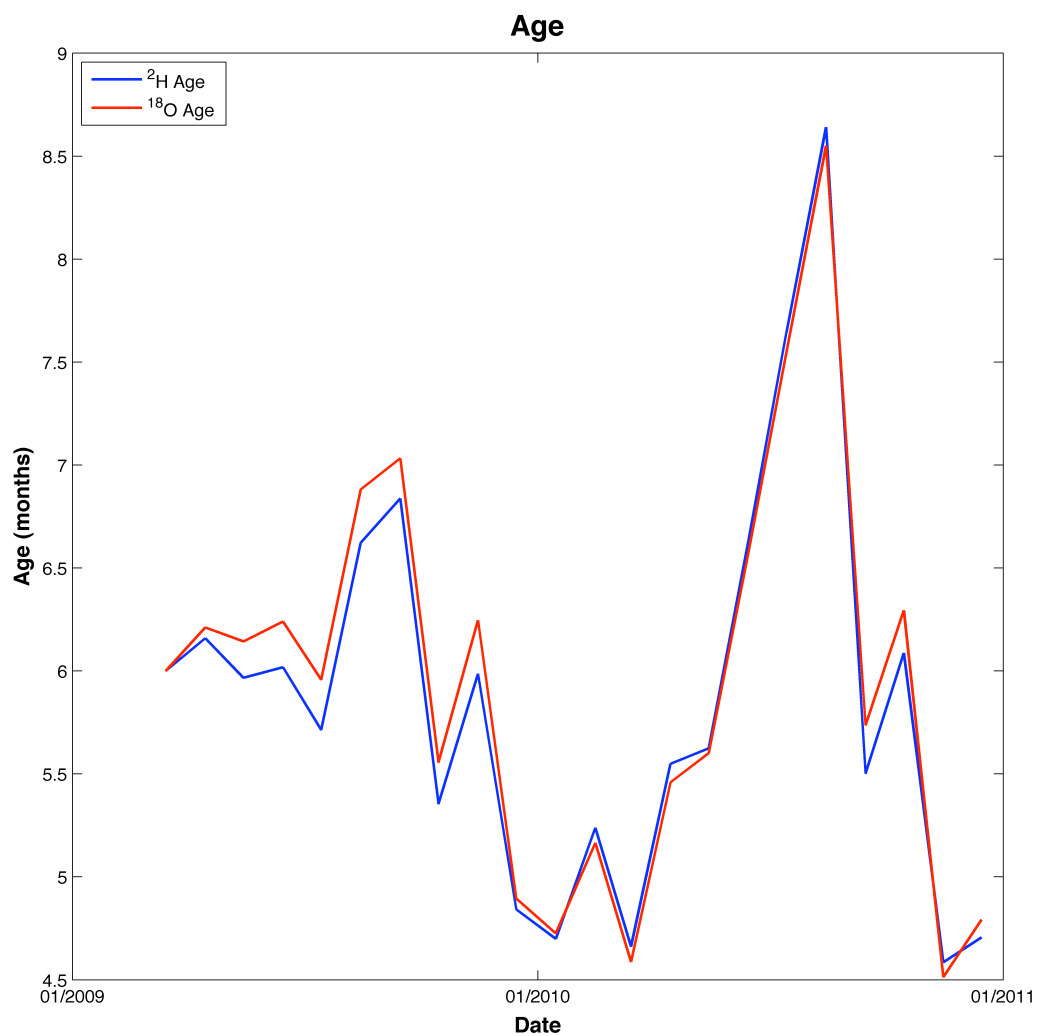


Figure 5-3. The solution to the piecewise constant inputs age model using the Shale Hills data. a. The modeled flow plotted with the measured flow. b. The modeled  $\delta^2\text{H}$  and  $\delta^{18}\text{O}$  concentrations plotted with the measured  $\delta^2\text{H}$  and  $\delta^{18}\text{O}$  concentrations. c. The mean age of the water stores in the system determined from the  $\delta^2\text{H}$  and  $\delta^{18}\text{O}$ .

## Chapter 6

### Conclusion

A  $\delta^2\text{H}$  and  $\delta^{18}\text{O}$  sampling network was implemented at the SSHCZO for the purposes of determining the flowpaths and timescales of the hydrologic pools. The precipitation was sampled on an event basis, soil water was sampled at approximately 80 locations weekly, groundwater was collected daily at two locations and weekly at 17 locations, and stream water was collected daily at the outlet. The preference for cold season infiltration and recharge was evident in means and the plotting of the data on the meteoric water line. The soil water and groundwater means were depleted relative to precipitation and the majority of points plotted above the lmwl, most likely due to fractionated snowmelt water (Clark and Fritz, 1997). Infiltration and recharge principally occurred over the period of late September – May, except for winter periods with frozen soils. Groundwater was likely recharged by macropores over this period when the soil was saturated. During the non-growing season the soil moisture is higher than during the growing season and therefore precipitation and snowmelt initiate macropore flow. Macropore flow would explain why the groundwater  $\delta^2\text{H}$  and  $\delta^{18}\text{O}$  mean is different from the precipitation. The groundwater occasionally flushed out the deepest soil water leaving behind its  $\delta^2\text{H}$  and  $\delta^{18}\text{O}$  signature in the soil. From the  $\delta^2\text{H}$  and  $\delta^{18}\text{O}$  means and the quantile ellipses it was found that streamflow was composed of approximately 67% groundwater and 33% surface runoff and soil water, possibly transported through preferential flowpaths.

Vegetation samples were collected for the purpose of determining where the trees were getting their water. These water samples were analyzed on the DLT-100, but it has been shown that there can be significant errors when analyzing samples with high organic content on the DLT-100 (West et al., 2010). Therefore the samples are also being analyzed on a mass spectrometer to determine how accurate the DLT-100 numbers are. When plotted on the lmwl

the  $\delta$  values from the DLT-100 plot in a different region than the soil water, groundwater or stream water, similar to the finding of Brooks et al. (2010). However, more work needs to be done to verify these results.

A piecewise constant input age model was developed based on the work of Duffy and Cusumano (1998) and Duffy (2010). The mean age of the water in the catchment was determined to be approximately 5-6 months for the period of January 2009 – December 2010. The age reached a maximum of approximately 9 months during the summer drought, and a minimum of approximately 4.5 months over the winter during recharge. While the age of the groundwater and soil water is likely different than 6 months, this serves as a good starting point. The next step for the age model will be to use it in a discrete model and to solve for the age of the mobile and immobile water.

The hydrologic functioning of the SSHCZO plays a role in all of the processes being studied there. Future studies can now use this information and see how it relates to the formation, evolution and function of the regolith

## References

- Allison G.B., Barnes C.J. (1983) Estimation of evaporation from non-vegetated surfaces using natural deuterium. *Nature* **301**. 143-145.
- Anderson S.P., Bales R.C., Duffy C.J. (2008) Critical Zone Observatories: Building a network to advance interdisciplinary study of Earth surface processes. *Mineralogical Magazine* **72**, 7-10.
- Araguas-Araguas L., Froelich K., Rozanski K. (2000) Deuterium and oxygen-18 isotope composition of precipitation and atmospheric moisture. *Hydrological Processes* **14**, 1341-1355.
- Baertschi P. (1976) Absolute  $^{18}\text{O}$  content of standard mean ocean water. *Earth and Planetary Science Letters* **31**, 341-344.
- Barnes C.J., Allison G.B. (1988) Tracing of water movement in the unsaturated zone using stable isotopes of hydrogen and oxygen. *Journal of Hydrology* **100**. 143-176.
- Bengtsson L., Saxena R.K., Dressie Z. (1987) Soil water movement estimated from isotope tracers. *Hydrological Sciences Journal* **32**. 497-520.
- Bergmann H., Sackl B., Maloszewski P., Stichler W. (1986) Hydrological investigations in a small catchment area using isotope data series. In *Proc. 5<sup>th</sup> Int. Symp. On Underground Water Tracing*, September 22-27, 1986, Athens. Institute of Geology and Mineral Exploration, Athens, pp. 255-272.
- Bolin B., Rodhe H. (1973) A note on the concepts of age distribution and transit time in natural reservoirs. *Tellus* **25**. 58-62.
- Brantley S.L., Goldhaber M.B., Vala Ragnarsdottir K. (2007) Crossing disciplines and scales to understand the Critical Zone. *Elements* **3**. 307-314.
- Brooks J. R., Barnard H. R., Coulombe R., McDonnell J. J. (2010) Ecohydrologic separation of water between trees and streams in a Mediterranean climate. *Nature Geoscience* **3**, 100-104.
- Brown V.A., McDonnell J.J., Burns D.A, Kendall C. (1999) The role of event water, a rapid shallow flow component, and catchment size in summer stormflow. *Journal of Hydrology* **217**. 171-190.
- Clark I. D., Fritz P. (1997) *Environmental Isotopes in Hydrogeology*. CRC Press, Florida.
- Craig H. (1961) Variations in meteoric waters. *Science* **133**, 1702-1703.
- Criss R.E., Davisson M.L. (1996) Isotopic imaging of surface water/groundwater interactions, Sacramento Valley, California. *Journal of Hydrology* **178**. 205-222.

- Danckwerts P.V. (1953) Continuous flow systems: Distribution of residence times. *Chemical Engineering Science* **2**. 1-13.
- Dansgaard W. (1964) Stable isotopes in precipitation. *Tellus* **4**, 436-468.
- Darling W.G., Bath A.H. (1988) A stable isotope study of recharge processes in the English chalk. *Journal of Hydrology* **101**. 31-46.
- Davisson M.L., Criss R.E. (1993) Stable isotope imaging of a dynamic groundwater system in southwestern Sacramento Valley, California, USA. *Journal of Hydrology* **144**. 213-246.
- De Wit J. C., Van Der Straaten C. M., Mook W. G. (1980) Determination of the absolute hydrogen isotopic ratio of V-SMOW and SLAP. *Geostandards Newsletter* **4**, 33-36.
- Deines P., Hull L.C., Stowe S.S. (1990) Study of soil and ground-water movement using stable hydrogen and oxygen isotopes. In. *Water Resources in Pennsylvania: Availability, Quality and Management* (ed. Majundar S.K., Miller E.W., Parizek R.R.) The Pennsylvania Academy of Science. pp. 121-140.
- Delhez E.J.M., Campin J.M., Hirst A.C., Deleersnijder E. (1999) Toward a general theory of the age in ocean modeling. *Ocean Modelling* **1**. 17-27.
- DeWalle D. R. and Swistock B. R. (1994) Causes of episodic acidification in five Pennsylvania streams on the northern Appalachian Plateau. *Water Resources Research* **30**, 1955-1963.
- Duffy C. J. (1996) A two-state integral-balance model for soil moisture and groundwater dynamics in complex terrain. *Water Resources Research* **32**, 2421-2434.
- Duffy C.J., Cusumano J. (1998) A low-dimensional model for concentration-discharge dynamics in groundwater stream systems. *Water Resources Research* **34**. 2235-2247.
- Duffy C.J. (2010) Dynamical modeling of concentration-age-discharge in watersheds. *Hydrological Processes* **24**. 1711-1718.
- Eriksson E. (1971) Compartment models and reservoir theory. *Annual Reviews Ecological Systems* **2**. 67-84.
- Friedman, I., Machta L., Soller R. (1962) Water-vapor exchange between a water droplet and its environment. *Journal of Geophysical Research* **67**, 2761-2766.
- Friedman I., Redfield A. C., Schoen B., Harris J. (1964) The variation of the deuterium content of natural water in the hydrologic cycle. *Reviews of Geophysics* **2**, 177-224.
- Gat J.R. (1971) Comments on the stable isotope method in regional groundwater investigations. *Water Resources Research* **7**. 980-993.
- Gat, J. R. (1996) Oxygen and hydrogen isotopes in the hydrologic cycle. *Annual Review of Earth and Planetary Science* **24**, 225-262.

- Gazis C., Feng X. (2004) A stable isotope study of soil water: evidence for mixing and preferential flow paths. *Geoderma* **119**. 97-111.
- Goode D.J. (1996) Direct simulation of groundwater age. *Water Resources Research* **32**. 289-296.
- Gourgue O., Deleersnijder E., White L. (2006) Toward a generic method for studying water renewal, with application to the epilimnion of Lake Tanganyika. *Coastal and Shelf Science* **74**. 628-640.
- Graham C., Lin H.S. (2011) Controls and frequency of preferential flow occurrence in the Shale Hills Critical Zone Observatory: A 175 event analysis of soil moisture response to precipitation. *Vadose Zone Journal* (in press).
- Hoefs J. (2009) *Stable Isotope Geochemistry*. Springer-Verlag, Berlin Heidelberg.
- Ingraham N. L., Criss R. E. (1993) Effects of surface area and volume on the rate of isotopic exchange between water and water vapor. *Journal of Geophysical Research* **98**, 20547-20553.
- Jin L., Ravella R., Ketchum B., Bierman P.R. Heaney P., White T., Brantley S.L. (2010) Mineral weathering and elemental transport during hillslope evolution at the Susquehanna Shale Hills Critical Zone Observatory. *Geochimica et Cosmochimica Acta* **74**. 3669-3691.
- Jin L., Andrews D.M., Holmes G.H., Duffy C.J., Lin H.S., Brantley S.L. (2011) Water chemistry reflects hydrological controls on weathering in Susquehanna Shale Hills Critical Zone Observatory (Pennsylvania, USA) (2011) *Vadose Zone Journal* (in press).
- Kirchner J.W. (2003) A double paradox in catchment hydrology and geochemistry. *Hydrological Processes* **17**. 871-874.
- Kuntz B. W. (2010) Laboratory, field, and modeling analysis of solute transport behavior at the Shale Hills Critical Zone Observatory. Masters thesis. Penn. State Univ.
- Lawrence J. R., Gedzelman S. D., White J. W. C., Smiley D., Lazov P. (1982) Storm trajectories in eastern US D/H isotopic composition of precipitation. *Nature* **296**, 638-640.
- Leaney F.W., Mettem K.R.J., Chottleborough D.J. (1993) Estimating the contribution of preferential flow to subsurface runoff from a hillslope using deuterium and chloride. *Journal of Hydrology* **147**. 83-103.
- Lin H. S. (2006) Temporal stability of soil moisture spatial pattern and subsurface preferential flow pathways in the Shale Hills Catchment. *Vadose Zone Journal* **5**, 317-340.
- Lin H. S., Kogelmann W., Walker C., Bruns M. A. (2006) Soil moisture patterns in a forested catchment: A hydropredological perspective. *Geoderma* **131**, 345-368.
- Lin H.S., Zhou X. (2008) Evidence of subsurface preferential flow using soil hydrologic monitoring in the Shale Hills catchment. *European Journal of Soil Science* **59**. 34-49.

- Lis G., Wassenaar L.I., Hendry M.J. (2008) High-precision laser spectroscopy D/H and  $^{18}\text{O}/^{16}\text{O}$  measurements of microliter natural water samples. *Anal. Chem.* **80**, 287-293.
- Lynch (1976) Effects of antecedent soil moisture on storm hydrographs. Ph. D. thesis, Penn. State Univ.
- Lynch J. A., Corbett E. S. (1989) Hydrologic control of sulfate mobility in a forested watershed. *Water Resources Research* **25**, 1695-1703.
- Maloszewski P., Zuber A. (1982) Determining the turnover time of groundwater systems with the aid of environmental tracers. 1. Models and their applicability. *Journal of Hydrology* **57**, 207-231.
- McDonnell J. J. (1990) A rationale for old water discharge through macropores in a steep, humid catchment. *Water Resources Research* **26**, 2821-2832.
- Merlivat L., Jouzel J. (1979) Global climatic interpretation of the deuterium-oxygen 18 relationship for precipitation. *Journal of Geophysical Research* **84**, 5029-5033.
- Nauman E. (1969) Residence time distribution theory for unsteady stirred tank reactors. *Chemical Engineering Science* **24**, 1461-1470.
- Nauman E. (1973) A note on residence time distributions in cyclic reactors. *Chemical Engineering Science* **28**, 313-315.
- O'Driscoll M. A., DeWalle D. R., McGuire K. J., Gburek W. J. (2005) Seasonal  $^{18}\text{O}$  variations and groundwater recharge for three landscape types in central Pennsylvania, USA. *Journal of Hydrology* **303**, 108-124.
- Pionke H. B., DeWalle D. R. (1992) Intra- and inter-storm  $^{18}\text{O}$  trends for selected rainstorms in Pennsylvania. *Journal of Hydrology* **138**, 131-143.
- Qu Y., Duffy C.J. (2007) A semidiscrete finite volume formulation for multiprocess watershed simulation. *Water Resources Research* **43**.
- Reich E.G. (1966) A rain study of a small drainage basin in Central Pennsylvania. Masters thesis. Penn State Univ.
- Rice K.C., Hornberger G.M. (1998) Comparison of hydrochemical tracers to estimate source contributions to peak flow in a small, forested, headwater catchment. *Water Resources Research* **34**, 1755-1766.
- Rozanski K., Araguas-Araguas L., Gonfiantini R. (1992) Relation between long-term trends of oxygen-18 isotope composition of precipitation and climate. *Science* **258**, 981-985.
- Sayama T., McDonnell J.J. (2009) A new time-space accounting scheme to predict stream water residence time and hydrograph source components at the watershed scale. *Water Resources Research* **45**.

- Sharp, Z. (2007) *Principles of Stable Isotope Geochemistry*. Pearson Prentics Hall, New Jersey.
- Siegenthaler U., Oeschger H. (1980) Correlation of  $^{18}\text{O}$  in precipitation with temperature and altitude. *Nature* **285**, 314-317.
- Sklash, M.G., Farvolden R.N. (1979) The role of groundwater in storm runoff. *Journal of Hydrology* **43**. 45-65.
- Sklash M.G., Farvolden R.N., Fritz P. (1976) A conceptual model of watershed response to rainfall, developed through the use of oxygen-18 as a natural tracer. *Canadian Journal of Earth Sciences* **13**. 271-283.
- Uhlenbrook S., Hoeg S. (2003) Quantifying uncertainties in tracer-based hydrograph separations: a case study for two-,three- and five-component hydrograph separations in a mountainous catchment. *Hydrological Processes* **17**. 431-453.
- Vogel T., Sanda M., Dusek J., Dohnal M., Votrubova J. (2010) Using oxygen-18 to study the role of preferential flow in the formation of hillslope runoff. *Vadose Zone Journal* **9**. 252-259.
- Werner T.M., Kadlec R.H. (1996) Application of residence time distributions to stormwater treatment systems. *Ecological Engineering* **7**. 213-234.
- West A.G., Goldsmith G.R., Brooks P.D., Dawson T.E. (2010) Discrepancies between isotope ratio infrared spectroscopy and isotope ratio mass spectrometry for the stable isotope analysis of plant and soil waters. *Rapid Communications in Mass Spectrometry* **24**. 1948 – 1954.
- Winograd I.J., Riggs A.C., Coplen T.B (1998) The relative contributions of summer and cool-season precipitation to groundwater recharge, Spring Mountains, Nevada, USA. *Hydrogeology Journal* **6**. 77-93.
- Zuber A. (1986) On the interpretation of tracer data in variable flow systems. *Journal of Hydrology* **86**. 45-57.

## Appendix

### $\delta^2\text{H}$ and $\delta^{18}\text{O}$ Data and Age Model Output

The  $\delta^2\text{H}$  and  $\delta^{18}\text{O}$  precipitation, soil water, groundwater and stream water data can be found at <http://www.czo.psu.edu/data.html>.

#### Age Model Output

Month	Flow (m <sup>3</sup> )	Stream $\delta^2\text{H}$	Stream $\delta^{18}\text{O}$	Age $\delta^2\text{H}$ (Months)	Age $\delta^{18}\text{O}$ (Months)
Jan 2009	3439.53				
Feb 2009	2173.90				
Mar 2009	1853.94				
Apr 2009	2703.45	- 52.93	- 8.35	6.16	6.21
May 2009	3922.37	- 50.89	- 7.88	5.97	6.14
Jun 2009	3365.83	- 50.17	- 7.73	6.02	6.24
Jul	3911.62	-	-	5.71	5.96

2009		50.42	7.72		
Aug		-	-		
2009	984.08	50.92	7.82	6.62	6.88
Sep		-	-		
2009	1726.00	51.38	7.97	6.84	7.03
Oct		-	-		
2009	6631.51	49.05	7.56	5.35	5.56
Nov		-	-		
2009	2693.46	48.32	7.43	5.99	6.25
Dec		-	-		
2009	5216.58	53.39	8.41	4.84	4.90
Jan		-	-		
2010	4852.85	53.99	8.49	4.70	4.73
Feb		-	-		
2010	2172.59	56.50	8.98	5.24	5.16
Mar		-	-		
2010	5187.30	57.33	9.04	4.66	4.59
Apr		-	-		
2010	1891.45	56.82	8.91	5.55	5.46
May		-	-		
2010	3279.54	55.33	8.53	5.62	5.60
Jun		-	-		
2010	825.06	55.54	8.58	6.63	6.57

Jul 2010	0.00			7.65	7.55
Aug 2010	0.00			8.64	8.55
Sep 2010	0.00			5.50	5.74
Oct 2010	0.00			6.09	6.29
Nov 2010	0.00			4.59	4.51
Dec 2010	0.00			4.71	4.79